AD_____

Award Number: DAMD17-03-1-0731

TITLE: Inhibition of Nitric Oxide Synthase through Depletion of its Cofactor Tetrahydrobiopterin as a Novel Strategy for Breast Cancer Anti-Angiogenic Therapy

PRINCIPAL INVESTIGATOR: Ines Batinic-Haberle, Ph.D.

CONTRACTING ORGANIZATION: Duke University Medical Center
Durham, NC 27710

REPORT DATE: September 2004

TYPE OF REPORT: Final

PREPARED FOR: U.S. Army Medical Research and Materiel Command
Fort Detrick, Maryland 21702-5012

REPORT DOCUMENTATION PAGE

Form Approved
OMB No. 074-0188

1. AGENCY USE ONLY (Leave blank)	2. REPORT DATE	3. REPORT TYPE AND DATES COVERED
	September 2004	Final (1 Sep 2003 - 31 Aug 2004)

4. TITLE AND SUBTITLE
Inhibition of Nitric Oxide Synthase through Depletion of its Cofactor Tetrahydrobiopterin as a Novel Strategy for Breast Cancer Anti-Angiogenic Therapy

5. FUNDING NUMBERS
DAMD17-03-1-0731

6. AUTHOR(S)

Ines Batinic-Haberle, Ph.D.

7. PERFORMING ORGANIZATION NAME(S) AND ADDRESS(ES)

Duke University Medical Center
Durham, NC 27710

E-Mail: ibatinic@duke.edu

8. PERFORMING ORGANIZATION REPORT NUMBER

9. SPONSORING / MONITORING AGENCY NAME(S) AND ADDRESS(ES)

U.S. Army Medical Research and Materiel Command
Fort Detrick, Maryland 21702-5012

10. SPONSORING / MONITORING AGENCY REPORT NUMBER

11. SUPPLEMENTARY NOTES

12a. DISTRIBUTION / AVAILABILITY STATEMENT
Approved for Public Release; Distribution Unlimited

12b. DISTRIBUTION CODE

13. ABSTRACT (Maximum 200 Words)

We showed previously that low molecular weight water-soluble antioxidant, manganese (III) tetrakis (*N*-ethylpyridinium-2-yl) porphyrin ($Mn^{III}TE\text{-}2\text{-}PyP^{5+}$) is effective catalyst for the elimination of reactive oxygen and nitrogen species in different rodent models of oxidative stress injuries. We further showed that this porphyrin can oxidize cellular reductants, among them redox cofactor of nitric oxide synthase (NOS), tetrahydrobiopterin, BH_4. It has been well-established that nitric oxide is essential for angiogenesis, stimulating endothelial cell proliferation in vitro. Tumors, being under oxidative stress, express iNOS, which leads to greatly increased levels of NO up to μM levels. Increased levels of BH_4 were thus required, and, reportedly, parallel increased NO production. When tetrahydrobiopterin is depleted NOS is inhibited and synthesizes superoxide rather than nitric oxide. We are testing here the hypothesis that depletion of BH_4 by $MnTE\text{-}2\text{-}PyP^{5+}$ would inhibit NOS, decrease NO levels and thus inhibit angiogenesis.

Within a scope of the project (Specific Aim 1), we showed that $MnTE\text{-}2\text{-}PyP^{5+}$, when given to mice caused drastic decrease in tumor vasculature density of 4T1 mammary carcinoma. We also defined the thermodynamics and kinetics of BH_4 reaction with $MnTE\text{-}2\text{-}PyP^{5+}$ (*Batinic-Haberle et al, 20024*), and adopted the HPLC method for measuring BH_4 and its oxidation product, 7,8-dihydrobiopterin in tumors.

14. SUBJECT TERMS
Breast Cancer

15. NUMBER OF PAGES
53

16. PRICE CODE

17. SECURITY CLASSIFICATION OF REPORT	18. SECURITY CLASSIFICATION OF THIS PAGE	19. SECURITY CLASSIFICATION OF ABSTRACT	20. LIMITATION OF ABSTRACT
Unclassified	Unclassified	Unclassified	Unlimited

Table of Contents

INTRODUCTION

Reactive oxygen (ROS) and nitrogen species (RNS). Reactive oxygen and nitrogen species (ROS and RNS) ($O_2^{\cdot-}$, $^{\cdot}NO$, $ONOO^-$, $ONOOCO_2^-$, $CO_3^{\cdot-}$, $NO_2^{\cdot}$, H_2O_2, $^{\cdot}OH$) either through direct oxidative damage or through signaling have been implicated in numerous pathological disorders such as carcinogensis, radiation injury, inflammation, ischemia/reperfusion, hemorrhagic shock, autoimmune diseases, neurologic disorders (amyotrophic lateral sclerosis, Parkinson disease, Alzheimer disease), stroke, spinal cord injury, and senescence [1].

ROS and cancer. ROS have been considered DNA-damaging agents that increase the mutation rate and promote oncogenic transformation. In addition to this unspecific action, reactive species produced in a regulated fashion are required participants in signaling pathways being involved in activation of activator protein-1, AP-1, hypoxia inducible factor, HIF-1 and nuclear factor NF-κB [2–8]. In addition to ROS, and depending upon its concentration, NO may affect HIF-1 activation also [7]. All of these transcription factors have predominant roles in development of cancer and metastasis. Consequently, ROS appear to be key regulatory factors in molecular pathways linked to tumor development and dissemination and thus likely targets in drug development.

Mn porphyrins and ROS and RNS. As a result of more than decade long efforts to synthesize potent catalytic antioxidants, our laboratory has developed structure-activity relationship between the ability of Mn porphyrins to eliminate $O_2^{\cdot-}$ (mimic SOD) and the redox property of the metal center, $E_{1/2}$ (Figure 1) [9-12]. Based on this relationship we have shown that, similar to the SOD enzyme itself, there is an optimal $E_{1/2}$ (showed in Figure 1 as a plateau of a bell shape curve), that allows Mn porphyrins to be efficient in dismuting $O_2^{\cdot-}$ [7]. That very same property enables them to be potent scavengers of peroxynitrite, carbonate radical and hydrogen peroxide. Based on this relationship we forwarded the Mn porphyrins of high and similar antioxidant potency, Mn(III) tetrakis(N-ethylpyridinium-2-yl)porphyrin, MnTE-2-PyP^{5+} (AEOL-10113) (***Scheme I***), and Mn(III) tetrakis(N,N-diethylpyridinium-2-yl)porphyrin, MnTDE-2-ImP^{5+} (AEOL-10150) for testing in different animal models of oxidative stress injuries where they invariably exhibited high protectiveness [13-22].

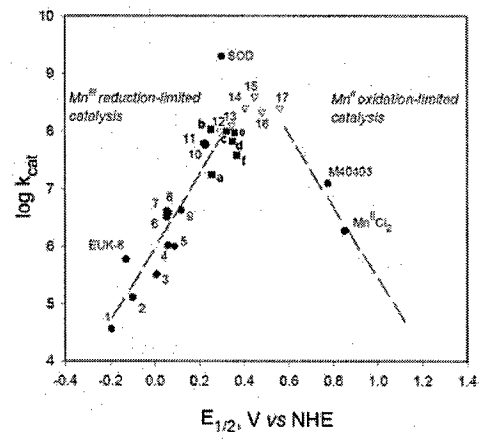

Figure 1. *Log k_{cat} for $O_2^{\cdot-}$ dismutation vs metal-centered redox potential, $E_{1/2}$ for Mn porphyrins, SOD, EUK-8 and M40403 (MnTE-2-PyP^{5+} is **11**, and MnTDE-2-ImP^{5+} is **d**) [9].*

Mn porphyrins and cellular reductants. In addition to eliminating reactive oxygen and nitrogen species, and for the very same reason of possesing an appropriate redox ability ($E_{1/2}$=+228 mV vs NHE), those porphyrins can be easily reduced by cellular

reductants also [16,23-26], as the redox state of a cell is highly reducing (E ~ -200mV vs NHE). Both Mn porphyrins where Mn is in its +3 and +4 oxidation state will be readily reduced. Therefore the harmful, highly oxidizing O=Mn^{IV}P (a product of the reaction of Mn^{III}P and $Mn^{II}P^{4+}$ with $ONOO^-$, $CO_3^{\cdot-}$ and H_2O_2) will be fastly eliminated. Moreover, while $Mn^{III}P^{5+}$ reduces $ONOO^-$ to $NO_2^{\cdot}$ radical, the $Mn^{II}P^{4+}$ will reduce ONOO through two electron transfer to unharmful species, nitrite NO_2^-. We have recently observed that in addition to glutathione and ascorbic acid Mn porphyrin can be reduced by tetrahydrobiopterin also [26]. The reduction product, $Mn^{II}P^{4+}$, is the same species as is formed in the reaction with ascorbic acid and glutathione. Because tetrahydrobiopterin is a redox cofactor of nitric oxide synthase, its depletion through its oxidation would result in NOS uncoupling and producing superoxide rather than nitric oxide. We therefore thought that oxidation of BH_4 by either $Mn^{III}P^{5+}$ or O=$Mn^{IV}P^{4+}$ may be physiologically relevant as it may decrease NO levels and affect angiogenesis. The effect may be relevant to tumor tissue where higher levels of iNOS are expressed and thus high levels of BH_4 are required.

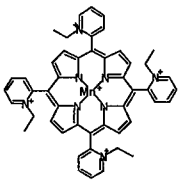

Mn^{III}TE-2-PyP^{5+}

Scheme I. Structure of the Mn(III) porphyrin studied

Mn porphyrins and transcription factors. Recently, new exciting data indicate that Mn porphyrins can inhibit activation of transcription factors (TF) by either interfering with ROS (preventing TF activation by ROS) or by oxidizing transcription factors directly. Thus, MnTE-2-PyP^{5+} was shown to inhibit DNA binding of AP-1, NF-κB and to suppress activation of HIF-1. All three factors are hypoxia-triggered and all three seem to be activated by ROS [27-30]. Of interest to note is that ROS generation by mitochondrial electron transport chain increases at lower [O_2], i.e. under hypoxic conditions [6]; thus mitochondria is suggested to act as an O_2 sensor.

NF-κB. The inhibition of NF-kB DNA binding has been explained in terms of oxidation of cysteine residue of p50 by MnTE-2-PyP^{5+} in nucleus [31]. Oxidation of cysteine residue resembles oxidation of glutathione by Mn(III) porphyrin that has been shown by us to occur [23]. The reaction is rather slow with Mn^{III}TE-2-PyP^{5+}. However, it occurs several orders of magnitude faster with O=$Mn^{IV}P^{4+}$ [23]. Aerobically reaction with glutathione essentially does not proceed at appreciable level; anaerobically the rate constant (room temperature) is ~ 3 x 10^2 M^{-1} s^{-1} [26]. Under aerobic conditions rate constant for the reaction of O=Mn^{IV}TM-2-PyP^{4+} with glutathione is 4 x 10^4 M^{-1} s^{-1} (37^oC) [23]. So the reaction of glutathione with O=Mn^{IV}P is at least 100-fold faster than with $Mn^{III}P^{4+}$. Thus a more likely scenario is that MnTE-2-PyP^{5+} will react with $ONOO^-$ (or with H_2O_2 or with $CO_3^{\cdot-}$) to form O=$Mn^{IV}P^{4+}$ which will be several orders of magnitude more reactive towards cysteine (of p50 subunit of NF-κB) as it is towards glutathione.

AP-1. It has been shown that MnTE-2-PyP^{5+} inhibits AP-1 activation leading to decreased number of metastasis in skin cancer. The number of total papillomas dropped from 31 to 5 when animals were treated 5 days per week for 14 weeks at 5 ng/mouse [32].

HIF-1α. Recently, MnTE-2-PyP^{5+} was reported to inhibit HIF-1 by scavenging ROS and/or RNS leading to significantly decreased tumor vasculature density [33,34].

Based on recent reports [31-34], MnTE-2-PyP^{5+} seems to be both a promising anticancer agent and an excellent tool for studying mechanism of cancerogenesis.

In this study we aimed at understanding: **(1)** whether MnTE-2-PyP^{5+} is anti-angiogenic and **(2)** whether its interaction with tetrahydrobiopterin, leading to decreased levels of NO contributes to its antiangiogenic effect. Since the start of this project, the new data indicated that MnTE-2-PyP^{5+} could affect NF-κB DNA binding and therefore iNOS expression and consequently levels of NO. Therefore we also aimed at distinguishing whether NO levels are decreased due to NOS inactivation (NOS activity assay) or to lower levels of NOS expression (Western blotting).

BODY OF THE PROJECT

Thermodynamic and kinetic characterization of BH_4 reaction with MnTE-2-PyP^{5+}

Tetrahydrobiopterin (***Scheme II***) is a co-factor of nitric oxide synthase [35,36],

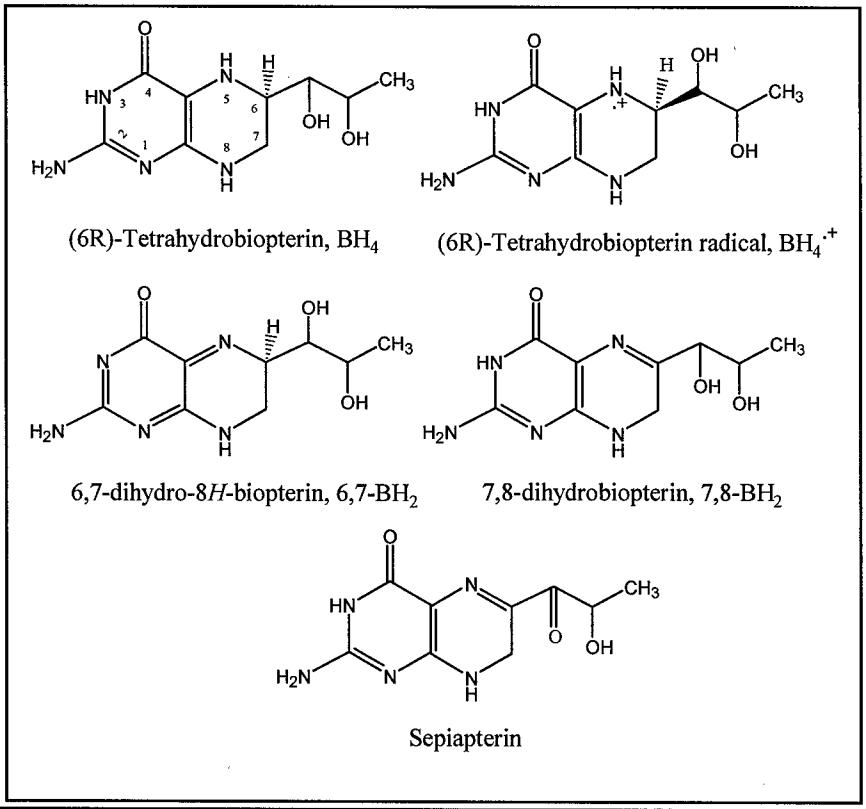

Scheme II. *Structures of tetrahydrobiopterin and its oxidized analogues*

and hence is an indirect regulator of vascular tone. The BH_4 appears to be essential for driving the synthesis of L-citrulline and NO formation by preventing the dissociation of the heme-Fe(II) dioxygen/heme-Fe(III) superoxide complex (thereby preventing the formation of superoxide), and by promoting the generation of heme-Fe(III) peroxo and heme-Fe(IV) oxo species (***Scheme III***) [37]. Only fully reduced tetrahydrobiopterin (and

not 7,8-BH_2) can support NOS catalysis [38,39]. Several *in vitro* studies directly established the role of ·NO and BH_4 in angiogenesis [40-44].

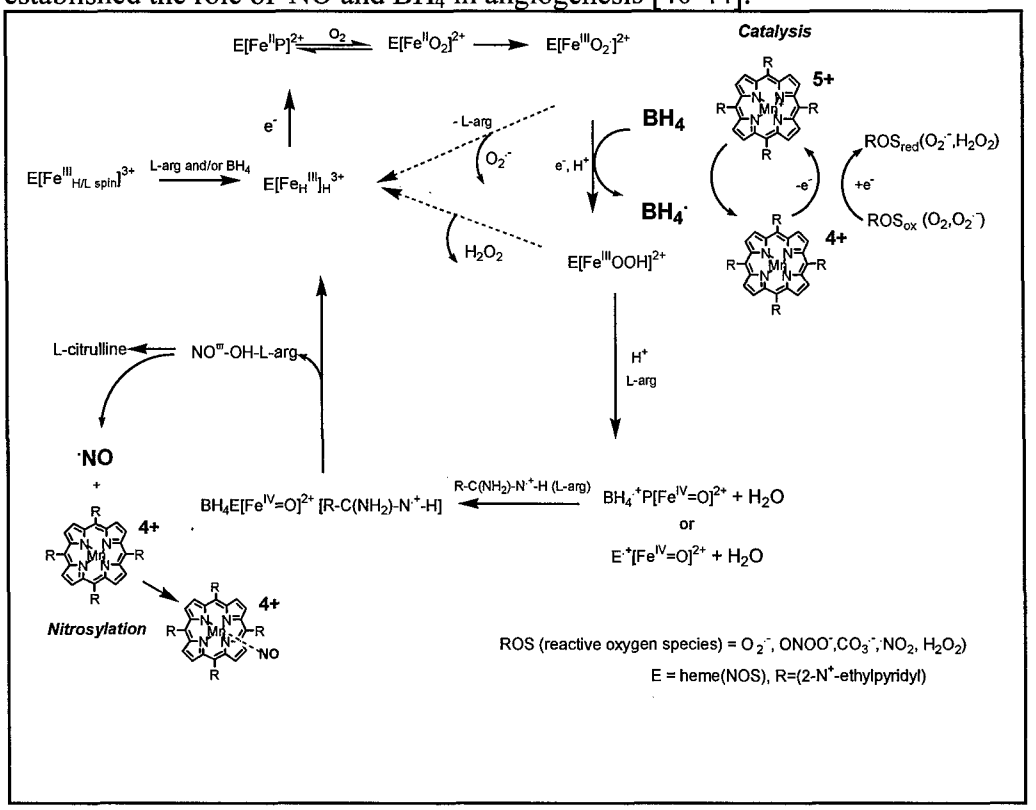

Scheme III. *Metalloporphyrin Inhibits Nitric Oxide Synthase (NOS) Through Depletion of its Cofactor, Tetrahydrobiopterin, BH4 which may affect NO-mediated cellular signaling*

Tumor tissue is under persistent oxidative stress with balance between cell proliferation and cell death shifted inappropriately toward excess proliferation, and with levels of antioxidants altered [45]. Both decreased and increased levels of superoxide dismutases, lower levels of catalase and lower levels of low-molecular weight antioxidants, such as ascorbic acid, uric acid and vitamin E have been reported in tumors [45-50]. Oxidative stress also results in over-expression of iNOS [40], accompanied by BH_4 levels higher than are found in normal tissue [48,49]. Due to the positive correlation between iNOS activity and tumor progression, iNOS inhibitors have been tested for cancer therapy [40]. In the tumor environment Mn porphyrins may selectively affect the levels of particular reductants, like BH_4, whose micromolar cellular levels [51,52] are much more sensitive to fluctuations than are the mM levels of glutathione and ascorbic acid. The catalytic depletion of BH_4 by MnTE-2-PyP^{5+} (Scheme III) would inhibit ·NO production by iNOS which in turn would impact signaling processes and angiogenesis. The depletion of BH_4 by H_2O_2-derived oxidized iron species (perferryl iron) in cerebellar granule neurons was observed by Kalyanaraman group [53], and it occurred presumably in a similar manner as with Mn(III) porphyrins. The BH_4 depletion resulted in production of $O_2^{\cdot-}$ by NOS rather than ·NO [53]. Mn porphyrin can be also reductively nitrosylated [54]. That reaction is however stoichiometric and at low oxygen levels fairly

irreversible. Thus it is unlikely that levels of nitric oxide would be affected through reductive nitrosylation of MnTE-2-PyP^{5+}.

We have shown in this work that tetrahydrobiopterin readily reduces Mn^{III}TE-2-PyP^{5+} (E in Figure 2), giving rise to Mn^{II}TE-2-PyP^{4+} (E+BH_4 in ***Figure 2***). We have also shown that 7,8-BH_2 can not be reduced back to BH_4 with ascorbic acid-reduced Mn^{II}TE-2-PyP^{4+}. Based on cyclic voltammetry, Gorren et al [55] reported that one-electron oxidation of BH_4 (as well as of tetrahydropterin) to $BH_4^{\cdot+}$ (at N 5, Scheme II) occurs at +270 mV *vs* NHE (pH 7.0). Using polarography, Archer et al [56] reported that reduced pterin (tetrahydropterin) undergoes reversible oxidation by two overlapping one-electron steps at +150 mV vs NHE (pH 7.0) producing 6,7-BH_2, which upon rearrangement gives rise to 7,8-BH_2. The authors [51] coupled the oxidation of pterin to the $Fe^{III}(CN)_6^{3-}/Fe^{II}(CN)_6^{4-}$ redox couple (E^o= + 358 mV *vs* NHE), whose reduction potential is similar to the potentials of Mn(III) porphyrins studied (+228 and +367 mV *vs* NHE for ethyl and n-octyl porphyrin, respectively, ref 11). In both studies, 7,8-BH_2 is the ultimate product of BH_4 oxidation. Based on the data reported [52,53], the two-step reduction of Mn^{III}TE-2-PyP^{5+} with BH_4 presumably occurs through eqs [1] and [2]:

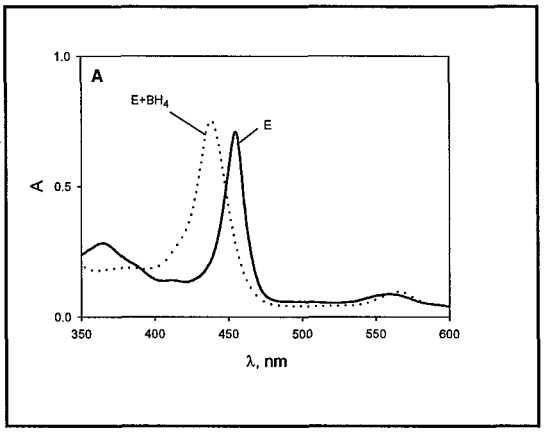

Figure 2. *The uv/vis spectra of oxidized, MnTE-2-PyP^{5+} (E) and BH_4-reduced MnTE-2-PyP^{4+} porphyrin (E + BH_4).*

$BH_4 + Mn^{III}T(alkyl)\text{-}2\text{-}PyP^{5+} <==> BH_4^{\cdot+} + Mn^{II}T(alkyl)\text{-}2\text{-}PyP^{4+}$ k_1 [1]

$BH_4^{\cdot+} + Mn^{III}T(alkyl)\text{-}2\text{-}PyP^{5+} <=> 6,7\text{-}(8H)\text{-}BH_2 + Mn^{II}T(alkyl)\text{-}2\text{-}PyP^{4+} + 2H^+$ k_2 [2]

6,7-(8*H*)-BH_2 <=====> 7,8-BH_2 [3]

We ascribed the k_1 (1.0×10^4 M^1 s^{-1}) to one-electron oxidation of BH_4 to $BH_4^{\cdot+}$

Figure 3. *Catalytic oxidation of BH_4 with 5 μM Mn^{III}TE-2-PyP^{5+} (E) in PBS, pH 7.4, at 25 ± 1°C. Catalytic action was enabled through reoxidation of Mn(II) porphyrin by oxygen.* ***Solid line:*** *In one experiment, first the 0.35 mM BH_4 was added into phosphate buffer followed by the addition of MnTE-2-PyP^{5+} as indicated. After ~200 s, and with MnTE-2-PyP^{5+}, another 0.73 mM BH_4 was added to assure that enough reductant was present. Finally, ~2 mg of $Na_2S_2O_4$ was added to assure removal of all oxygen.* ***Dash line:*** *In another experiment, first 5 μM MnTE-2-PyP^{5+} (E) was added into phosphate buffer, followed by the addition of 0.9 mM BH_4 as indicated. Finally, ~ 2mg of $Na_2S_2O_4$ was added as noted.*

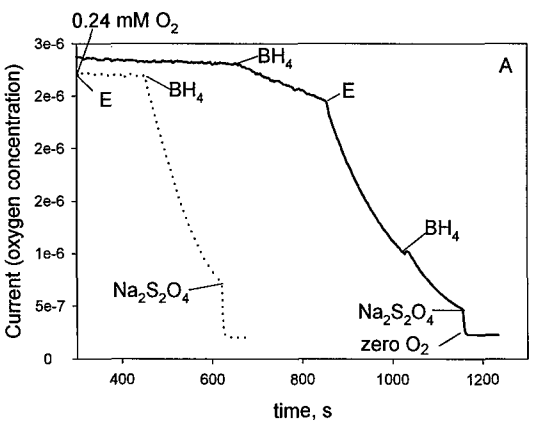

radical (eq 1), and k_2 (1.5×10^3 M^1 s^{-1}) to the one electron oxidation of $BH_4^{\cdot+}$ to 6,7-(8*H*)-BH_2 (eq 2). As was the case with ascorbic acid, glutathione and uric acid, reductive nitrosylation of Mn^{III}TE-2-PyP^{5+} occurs readily in the presence of both BH_4 and $^{\cdot}NO$.

Moreover, Mn^{III}TE-2-PyP^{4+} oxidizes tetrahydrobiopterin in a catalytic manner aerobically (***Figure 3***).

As previously discussed in relation to NF-κB, it is even more likely that $O{=}Mn^{IV}P^{4+}$ formed in the reaction of $Mn^{III}P^{4+}$ with $ONOO^-$, H_2O_2, and $CO_3^{\cdot-}$, would react with BH_4. Based on glutathione reactivity towards $O{=}Mn^{IV}P^{4+}$ and $Mn^{III}P$ [23,26] (discussed under NF-κB) we may predict that the rate constant of $O{=}Mn^{IV}P^{4+}$ with BH_4 would be $>>10^6$ M^{-1} s^{-1}.

Thermodynamic and kinetic characterization of the reaction of MnTE-2-PyP^{5+} with BH_4 and 7,8-BH_2 was published in *Free Radic. Biol. Med.* 2004 [26].

HPLC determination of BH_4 and 7,8-dihydrobiopterin

HPLC method for determination of BH_4 and 7,8-BH_2 is based on differential oxidation of these two compounds under basic and acidic conditions. Three methods were tested and partly employed for our conditions.

The method has been originally developed by Fukushima and Nixon [57], and modified [58,59], it is widely used for BH_4 and 7,8-BH_2 determination in different biological tissues. It is based on the oxidation of these compounds in acid and base medium by iodide followed by the reduction of excess iodide by ascorbic acid. Both BH_4 and 7,8-BH_2 are oxidized to biopterin in the acid (pH~1). In base (pH ~13) only 7,8-BH_2 was oxidized to biopterin, while BH_4 was oxidized to pterin. The oxidation of BH_4 to biopterin in acidic medium occurs over quinoid dihydrobiopterin that tautomerizes to 7,8-BH_2, which loses proton on C-6 of the pterin ring (*Scheme II*) that finally leads to the formation of biopterin [61-64]. Under alkaline conditions, loss of proton from the side chain on C'-1 hydroxyl (*Scheme II*) is favored [61], which results in a loss of side chain, i.e. formation of pterin. BH_4 appears to be sensitive to light, oxygen, traces of metal and pH of the solution [60]. Thus solid BH_4 is kept in freezer at -20 ^{0}C while its stock solution was prepared in 20 mM HCl/1 mM EDTA and was kept in refrigerator for up to 24 hours. Biopterin is a stable, fully oxidized pterin. Its stock solution was prepared in 2 mM NaOH because it was not soluble in water. Any attempt to concentrate the sample on Dowex 50 as indicated by Fukushima and Nixon [57] lead to nearly full retention of biopterin on column. No significant recovery of the biopterin from column was possible. Dithioerythritol (DTE) was added to the tissue homogenate to prevent loss of BH_4 during homogenization [58] and did not seem to rereduce 7,8-BH_2 to BH_4. Addition of DTE required higher concentration of ascorbic acid in order to eliminate excess of both DTE and iodine.

Several methods were eventually tested, some of them failed to give sensitive and reproducible chromatograms. Finally the method by Fiege at al [58] was adopted with minor modifications. ***Calibration curve for BH_4*** was made as follows. Primary BH_4 standards (0.5 mg/kg) were kept in 20 mM HCl/1 mM EDTA. Primary biopterin standards (0.5 mg/kg) were kept in 2 mM NaOH. Primary standard was diluted 100-fold with water to give secondary standard of concentration 5 μg/mL. To different volumes of BH_4 secondary standard solutions, appropriate volumes of 0.1 M phosphoric acid was

added to a total volume of 1 mL. The BH_4 concentrations ranged from 10 to 200 ng/mL. For acidic oxidation, to BH_4/phosphoric acid solutions the 0.11 mL of 2M trichloroacetic acid (TCA) was then added followed by 50 μL of aq 5% J_2/10% KJ. After 1 hour of oxidation in dark at room temperature, 50 μL of aq 5% ascorbic acid and 310 μL of water were added. For basic oxidation, to BH_4/phosphoric acid solutions the 0.11 mL of 2M NaOH, 50 μL of aq 5%J_2/10%KJ was added, left 1 hour in dark, 50 μL of 5% ascorbic acid and 310 μL of 1.42 M TCA. We assured that both solutions have similar acidity, becvause we showed that the retention time of biopterin on column is pH dependent. The 150 μL of these solutions were injected into Waters 2695 HPLC system with Waters 474 scanning fluorescence detector, with Whatman Partisil 10 μm particle size (250 x 4.6 mm) ODS-2 column and 95 % 10 mM phosphate buffer, 5 % methanol as a mobile phase, pH 6.4, 2mL/min flow. The excitation was set to 350 nm and emission to 450 nm. Usually more iodine is needed for oxidation under alkaline than under basic conditions [57].

Tissue analysis on BH_4: 1.8 g of fibrosarcoma was homogenized under ice and under argon in 5.5 mL of 0.1 M phosphoric acid to which 5 mM DTE was added (7.7 mg/10 mL 0.1 M phosphoric acid, 0.077% [58]). The 1 mL of homogenate was taken for alkaline and acidic oxidations. The 0.11 mL of 2M TCA and 100 μL of 5%J_2/10% KJ was added to acidic and 0.11 mL of 2.5 M NaOH and 100 μL 5% J_2/10% KJ to basic solution. Both solutions were left in dark for one hour. Then 100 μL of 5% ascorbic acid is added to both solutions, and 310 μL of water to acidic solution and 310 μL of 1.6 M TCA to basic solution, respectively. Both solutions were then centrifuged twice and filtered using ultrafilters 10,000 MW cut-off (5 000 g for 30 minutes). The 150 μL of filtrate was injected into HPLC. Different concentrations of ascorbic acid, DTE, and iodine (and the lack of them) were tested and the above amounts are those finally chosen to provide best results.

Nitric oxide synthase. The ^{14}C-arginine to ^{14}C-citrulline conversion leading to NO production as a method for NOS activity measurements [65-68] has not yet been tested. In addition to activity assay Western blotting will be performed.

Study of the effect of MnTE-2-PyP^{5+} on rodent tumor angiogenesis.

Preliminary data indicated that there is a significant tumor growth delay upon treatment of mice and rats with Mn porphyrin. Thus, subcutaneous B16 mouse melanoma and R3230 rat mammary adenocarcinoma were established in C57B/16 mice and Fischer-344 rats, respectively. Tumors were allowed to reach 8 mm in diameter before animals were randomized to the MnTE-2-PyP^{5+} (AEOL-10113) treated (6 mg/kg, IP, daily) or control (PBS, IP, daily). The MnTE-2-PyP^{5+} treated group experienced tumor growth delay (time to reach 5X initial tumor volume of 5 days) for both tumor models, verifying that Mn porphyrin has anti-tumor activity (***Figures 4 and 5***).

Figure 4. *R3230 tumor growth delay upon treatment of rats with MnTE-2-PyP^{5+} (AEOl-10113) at 6 mg/kg/daily. The growth curves are plotted as the mean relative treatment group tumor value +/- standard error. Mean times to reach 5-times initial tumor volume for each group were calculated and compared using the non parametric Kruskal-Wallis and Mann Whitney tests.*	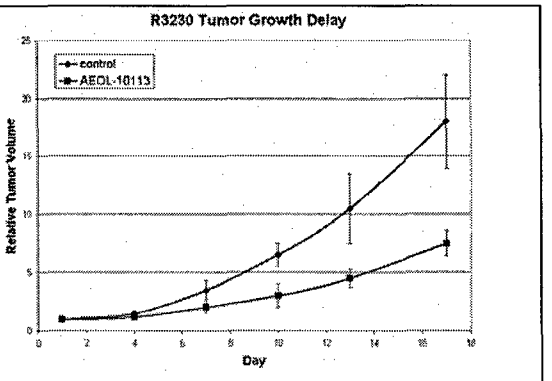
Figure 5. *4T1 tumor growth delay in MnTE-2-PyP^{5+} treated mice with 6 mg/kg/daily. The growth curves are plotted as the mean relative treatment group tumor value +/- standard error. Mean times to reach 5-times initial tumor volume for each groupwere calculated and compared using the non parametric Kruskal-Wallis and Mann Whitney tests.*	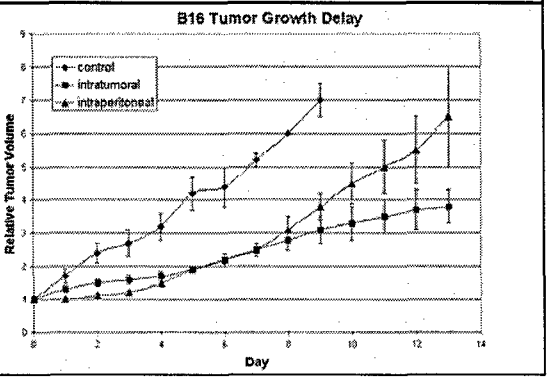

Next, plexiglass chambers containing a mixture of fibrin and R3230 cells were implanted subcutaneously in Fischer-344 rats, followed by randomized treatment as stated above. Tumor tissue was then removed and analyzed immunohistochemically for vascular density, revealing significant ($p<0.01$) inhibition of vascularization in MnTE-2-PyP^{5+} treated tumors.

In this project we established tumors on 8 to 10-week-old mice in dorsal skinfold window chambers [69,70], shown in ***Figure 6,*** by injecting 4T1 mouse mammary carcinoma cells expressing hypoxia-responsive green fluorescent protein, serving as a reporter of HIF-1α activity. Mice were treated 6 mg/kg/daily, IP once tumors reached 3 mm in diameter. Tumor growth and vascularity were not different between treated and non-treated animals for the first 10 days following transplantations. Between days 10 and 12 however a significant ($p<0.001$) decrease in microvascular density was observed in treated tumors with many becoming completely avascular. A representative image of the effect of MnTE-2-PyP^{5+} on decreasing vascular density is shown in ***Figure 7.*** This vascular destabilization was followed by a significant ($P<0.01$) reduction in tumor

Figure 6. *Dorsal skinfold window chamber.*	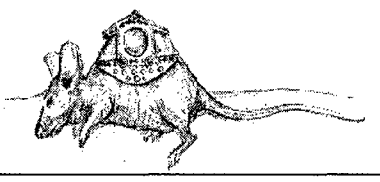

diameter in treated group. There were no significant differences in global tumor HIF-1α reporter gene activity levels between treated and control groups. These results suggest that MnTE-2-PyP^{5+} inhibits tumor growth largely by causing vascular destabilization.

Also these data imply that anti-vascular activity is either not related to HIF-1α or related to HIF-1α down-regulation in limited tumor regions undetectable by the methodology used here.

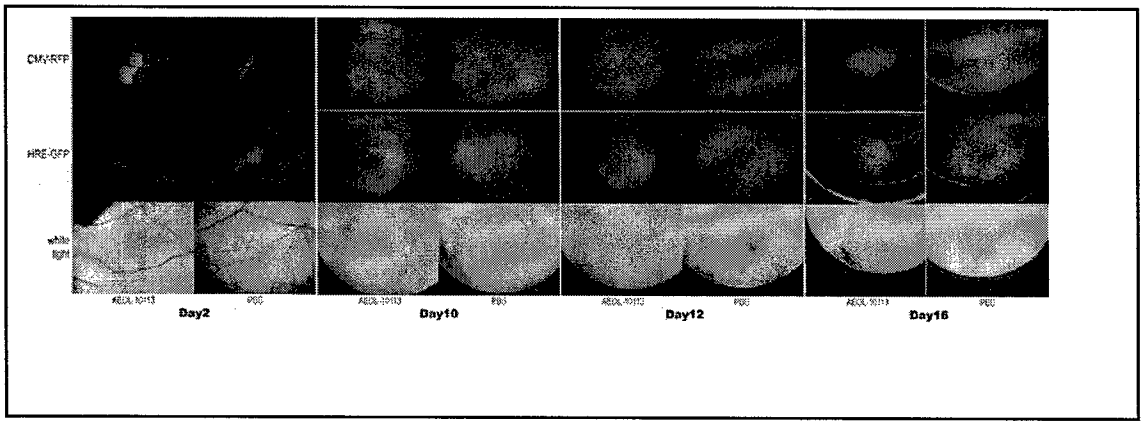

Figure 7. *Visualization of tumor and HIF-1α in MnTE-2-PyP^{5+} (6 mg/kg/daily, IP) treated mice. CMV-RFP is a construct introduced into tumor that allows expression of red fluoresecence protein (RFP) of a cytomegalovirus (CMV) promoter so that tumor cells can be tracked. The 4T1 line expresses hypoxia responsive green fluorescent protein serving as a reporter for HIF-1α.*

Study of the MnTE-2-PyP^{5+}/radiation on rodent tumor angiogenesis

Meanwhile another study has been finished that indicated that significant tumor devascularization occurs within 48 days of MnTE-2-PyP^{5+} + radiation treatment of mice [34]. Mice have tumors grown in dorsal skinfold window chambers and were randomized to **(1)** treatment with porphyrin (6 mg/kg, IP) at 0, 24 and 48 hours, **(2)** to radiation only, **(3)** to MnTE-2-PyP^{5+} + radiation and **(4)** to PBS treatment. Data are shown in ***Figure 8***. As

Figure 8. *The window chamber tumors were randomized to treatment with PBS or MnTE-2-PyP^{5+}, and radiation or sham-irradiation. A course of three fractions of radiation (5 Gy each, 12 hours apart) was followed immediately by daily administration of MnTE-2-PyP^{5+} (6 mg/kg) for three days. Tumors were imaged immediately after radiation (0 hours), and every day thereafter (24, 48, and 72 hours), and these images were used to calculate the tumor vascular length densities. Combined treatment resulted in significant tumor devascularization between 48 and 72 hours post-radiation. n = 5/group. * = P < 0.05 vs. "0 hour" tumor VLD.*

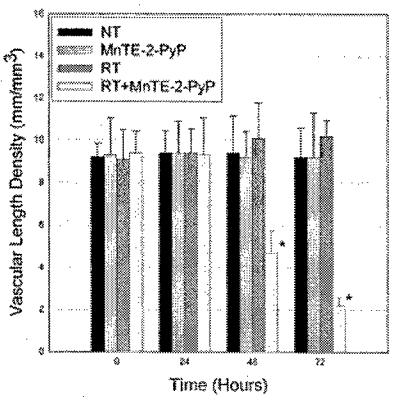

expected tumor vasculature did not show any change within 72 hours with MnTE-2-PyP^{5+} treatment only (note that in ***Figure 7***, antiangiogenic effects start to appear *not before the 10th day* after MnTE-2-PyP^{5+} treatment). Also, no change was observed with radiation treatment only. However there was a slight tendency towards increased vascular density presumably due to HIF activation. Yet, when MnTE-2-PyP^{5+} was given immediately after radiation there was a fast and drastic decrease in tumor vasculature at 48 hours, and is even more pronounced at 72 hours. This effect is explained in terms of radiation-induced, reactive oxygen species-dependent inactivation of HIF-1α. Consequently, the expression of a variety of cytokines would be suppressed among them VEGF and bFGF that would lead to tumor shrinkage (Moeller at al, submitted [33], manuscript enclosed). In the absence of MnTE-2-PyP^{5+} tumor cells are secreting cytokines that allow endothelial cells to be radioresistant [33]. If tumor cells are cultured with Mn porphyrin, and such conditioned media is added to adherent endothelial cells before radiation, upon radiation endothelial cells become much less viable as compared to the conditions were no MnTE-2-PyP^{5+} was present [33].

Study of the MnTE-2-PyP^{5+}/radiation on HIF-1 activation in rodent tumor angiogenesis

Recently, our group (Moeller et al, Cancer Cell, 2004, enclosed) reported the unambiguous evidence that HIF-1 is ROS (established either by direct addition of H_2O_2, or by addition of NO or by radiation) activated and that potent scavenger of ROS, as is MnTE-2-PyP^{5+}, is able to inactivate HIF-1 (when given immediately after radiation for three days at 6 mg/kg, IP, every 24 hours, three doses in total). Consequently, the decrease in levels of cytokines VEGF, and bFGF was detected which leads to the decrease in tumor vasculature density [34].

KEY RESEARCH ACCOMPLISHMENTS

We **fully characterized BH_4 and 7,8-BH_2 reactions with Mn porphyrins**. While we initially thought $Mn^{III}P/Mn^{II}P$ redox may be coupled to BH_4/7,8-BH_2 couple, few orders of magnitude faster reaction might occur employing $Mn^{III}P/O{=}Mn^{IV}P$ redox couple. The reactivity of $ONOO^-$-produced $O{=}Mn^{IV}P^{4+}$ towards BH_4 should be studied.

We determined that **MnTE-2-PyP^{5+} causes anti-angiogenesis** both in the presence and absence of radiation. However, in the presence of radiation the effect is significantly more pronounced.

In the absence of radiation treatment, the antiangiogenic effect started to appear after 12 days of daily MnTE-2-PyP^{5+}-treatment with 6 mg/kg mouse, and seems not to be HIF related because *levels of HIF-1 α were not affected.*

When MnTE-2-PyP^{5+} was given shortly after radiation (as a part of a separate project within Radiation Oncology Department), HIF-1 was fully inactivated presumably due to the ROS scavenging ability of MnTE-2-PyP^{5+}. The data indicate that **VEGF and bFGF were secreted by tumor cells in concert with high HIF-1α activity. Consequently, elimination of ROS (produced as a result of radiation) by MnTE-2-PyP^{5+} inactivates HIF-1α, prevents cytokine expresssion and leads to tumor**

shrinkage after 72 hours of treatment (6 mg/kg, IP, at 0, 24, and 48 hours). These events are presumably in the origin of tumor growth delay.

It may be speculated that in the absence of radiation, angiogenesis occurs through different mechanism/s that may include **(1)** other transcription factors (AP-1, NF-κB) and expression of genes such as (iNOS, COX-2, PGE_2); and/or **(2)** NOS inhibition through BH_4 depletion.

Problems. We were not able to finalize our project but we hope to do so within another several months. We responded to Specific aim 1. While we already adjusted BH_4 assay for tumors, we are still in a process of modifying NOS activity assay and NOS expression method for studying tumors. Once the methods are adjusted for our conditions, we will grow tumors in mice (in the presence and absence of MnTE-2-PyP^{5+} (6 mg/kg/daily, IP). When tumors reach 5-fold initial size we will analyze them for BH_4 and NOS content and activity, respectively (Specific aim 2).

REPORTABLE OUTCOME

Published. A manuscript has been published in *Free Radic. Biol. Med.,* 2004, characterizing reaction of BH_4 and 7,8-BH_2 with MnTE-2-PyP^{5+}. The manuscript also includes the proposed mechanism for anti-angiogenesis, and discussion-related to it [26].

Submitted. A manuscript related to the anti-angiogenic effect of MnTE-2-PyP^{5+} in the presence of radiation has been submitted for publication in *Int. J. Rad. Oncol. Biol. Phys.*, 2004 [33].

In preparation. Manuscript related to the anti-angiogenic effect of MnTE-2-PyP^{5+} alone is in preparation.

Submitted. A manuscript has been submitted for publication in *Cancer Res.* by Zhao et al, where IBH is a co-author and acknowledges financial help received in this period from DOD for cancer-related research.

Presentations. Work has been in part presented at *Gordon Conference on Oxygen Radicals* in Ventura, 2004, and will be presented at *11th Annual Meeting of Society for Free Radical Biology and Medicine* in St. Thomas, Virgin Islands 2004.

CONCLUSIONS

Our study as well as the data from two other studies summarized herein, indicate that ***MnTE-2-PyP^{5+} has exceptional potential as an anti-angiogenic compound.*** Our study of BH_4 /MnTE-2-PyP^{5+} system also indicate that Mn^{III}TE-2-PyP^{5+} reacts with BH_4, redox cofactor of NOS, and by depleting it may inhibit NOS and decrease levels of NO leading to decreased angiogenesis. The effect may be even more significant with $ONOO^-$ -oxidzed O=Mn^{IV}TE-2-PyP^{4+}.

When given along with radiation, MnTE-2-PyP^{5+} seems to cause anti-angiogenesis by scavenging ROS so that HIF-1 can not be activated, VEGF and bFGF not expressed and neovascularization supressed.

However, when MnTE-2-PyP^{5+} was given alone, the mechanism of angiogenesis appears to be independent of HIF-1 activation, and may be related to BH_4 depletion

and/or NF-κB and AP-1 inactivation. Thus antiangiogenic effects may be exerted through the suppression of NF-κB-driven target gene activation, such as through the COX-2 gene and PGE_2 (prostaglandin) signaling pathways [27]. These in turn were reported to modulate VEGF expression negatively at both the RNA and protein levels of VEGF and also restrict cellular aggregation and tube formation associated with angiogenesis and neovascularization.

Thus, recent findings related to MnTE-2-PyP^{5+} along with our work and related reports, suggesting a complexity of angiogenesis and mechanism/s of porphyrin in vivo action/s, prone us to extend our project/s. In addition to study the levels of NOS and BH_4, we are planning to investigate the response of all three transcriptions factors and targeted genes to MnTE-2-PyP^{5+} +/- radiation treatment.

ABBREVIATIONS

MnP, any Mn porphyrin (bold numbers and letters are related to Figure 1); Mn^{III}T(alkyl)-2-PyP^{5+}, Mn(III) *meso* tetrakis(*N*-alkylpyridinium-2-yl)porphyrin; alkyl being methyl (**10**) (M), ethyl (**11**) (E) (AEOL-10113), n-butyl (**a**) (nBu), n-hexyl (nHex) and n-octyl (nOct); Mn^{III}TDE(M)-2-ImP^{5+} (**c,d**) (DE, DM), Mn(III) *meso* tetrakis[*N,N'*-diethyl(dimethyl)imidazolium-2-yl]porphyrin (AEOL-10150), (**7**) MnTM-3-PyP^{5+}, Mn(III) *meso* tetrakis(*N*-methylpyridinium-3-yl)porphyrin; (**8**) MnTM-4-PyP^{5+}, Mn(III) *meso* tetrakis(*N*-methylpyridinium-4-yl)porphyrin; (**6**) Mn^{III}BM-2-PyP^{3+}, Mn(III) 5,10-bis(2-pyridyl)-15,20-bis(*N*-methylpyridinium-2-yl)porphyrin; (**9**) Mn^{III}TrM-2-PyP^{4+}, manganese(III) 5-mono-(2-pyridyl)-10,15,20-tris(*N*-methylpyridinium-2-yl)porphyrin; (**2**) Mn^{III}T(TMA)P^{5+}, manganese(III) *meso* tetrakis(*N, N, N*-trimethylanilinium-4-yl)porphyrin; (**4**) Mn^{III}T(TFTMA)P^{5+}, manganese(III) *meso* tetrakis(2,3,5,6-tetrafluoro-*N, N, N*-trimethylanilinium-4-yl)porphyrin; (**1**) Mn^{III}TCPP^{3-}, manganese *meso* tetrakis(4-carboxylatophenyl)porphyrin; Mn^{III}TSPP^{3-}, manganese(III) *meso* tetrakis(4-sulfonatophenyl)porphyrin; (**5**) Mn^{III}T(2,6-Cl_2-3-SO_3-P)P^{3-}, manganese(III) *meso* tetrakis(2,6-dichloro-3-sulfonatophenyl)porphyrin; (**3**) Mn^{III}T(2,6-F_2-3-SO_3-P)P^{3-}, manganese(III) *meso* tetrakis(2,6-difluoro-3-sulfonatophenyl)porphyrin; (**12-15**) $Mn^{II}Cl_{1-5}$TE-2-PyP^{4+}, Mn(II) β-mono-, di-, tri-, tetra-, pentachloro *meso* tetrakis(*N*-ethylpyiridinium-2-yl)porphyrin; (**16**) $Mn^{II}Br_8$TM-4-PyP^{4+}, Mn(II) β-octabromo *meso* tetrakis(*N*-methylpyridinium-4-yl)porphyrin; Mn^{III}TMOE-2-PyP^{5+} (**b**) (MOE), Mn(III) *meso* tetrakis[*N*-(2-methoxyethyl)pyridinium-2-yl]porphyrin; Mn^{III}TM,MOE-2-ImP^{5+} (**e**) (M,MOE), Mn(III) *meso* tetrakis[*N*-methyl-*N'*-(2-methoxyethyl)imidazolium-2-yl]porphyrin; Mn^{III}TDMOE-2-ImP^{5+} (**f**) (DMOE), Mn(III) *meso* tetrakis[*N,N'*-di(2-methoxyethyl)imidazolium-2-yl]porphyrin; EUK-8, Mn(III) salen; M40403, Mn(II) cyclic polyamine; NHE, normal hydrogen electrode; SOD, superoxide dismutase; M9CA, M9 casamino acids medium. BH_4-tetrahydrobiopterin; 7,8-BH_2, 7,8-dihydrobioptrein; AP-1, activator protein-1; NF-κB, nuclear factor NF-κB; HIF-1α, hypoxia-inducible factor 1α.

REFERENCES

1. Halliwell, B., Gutteridge, J., *Free radicals in biology and medicine*. New York, Oxford University Press, 1999. Batinic-Haberle, I.; Spasojevic, I.; Stevens, R. D.; Hambright, P.; Neta, P.; Okado-Matsumoto, A.; Fridovich, I. New class of potent catalysts of $O_2^{\bullet-}$ dismutation. Mn(III) methoxyethylpyridyl- and methoxyethylimidazolylporphyrins. *J. Chem. Soc. Dalton Trans.* 1696-1702; 2004.
2. Behrend, L., Henderson, G., Zwacka, R. M., Reactive oxygen species in oncogenic transformation, *Biochem. Soc. Trans.* **31**: 1442-1444; 2003.
3. Obereley, T. D., Oxidative damage in cancer, *Am. J. Pathol.* **160**: 403-408; 2002.
4. Klaunig, J. E., Kamendulis, L. M., The role of oxidative stress in carcinogenesis, *Annu. Rev. Pharmacol. Toxicol.* **44**: 239-267; 2004.
5. Nelson, K. K., Melendez, J. A., Mitochondrial redox control of matrix metalloproteinases, *Free Radic. Biol. Med.* **37**: 768-784; 2004.

6. Chandel, N. S., McClintock, D. S., Feliciano, C. E., Wood, T. M., Melendez, J. A., Rodriguez, A. M., Schumacker, P. T., Reactive oxygen species generated at mitochondrial complex III stabilize hypoxia-inducible factor-1a during hypoxia, *J. Biol. Chem.* **275**: 25130-25138; 2000.
7. Mateo, J., Garcia-Lecea, M., Cadenas, S., Hernandez, C., Moncada, S., Regulation of hypoxia-inducible factor 1-alpha by nitric oxide through mitochondria-dependent and –independent mechanisms, *Biochem. J.* 376: 537-544; 2003.
8. Wellman, T. L., Jenkins, J., Penar, P. L., Tranmer, B., Zahr, R., Lounsbury, K. M., Nitric oxide and reactive oxygen species exert opposing effects on the stability of hypoxia-inducible factor 1-alpha (HIF-1alpha) in explants of human pial arteries., FASEB J. 18: 379-381; 2003.
9. Batinic-Haberle, I., Spasojevic, I., Stevens, R. D., Hambright, P., Fridovich, I., Manganese(III) *meso*-tetrakis(*ortho*-*N*-alkylpyridyl)porphyrins. Synthesis, characterization, and catalysis of $O_2^{\cdot-}$ dismutation, *J. Chem. Soc. Dalton Trans.* 2689-2696; 2002.
10. Batinic-Haberle, I., Benov, L., Spasojevic, I., Fridovich, I., The *ortho* effect makes manganese(III) meso-tetrakis(N-methylpyridinium-2-yl)porphyrin a powerful and potentially useful superoxide dismutase mimic, *J. Biol. Chem.* **273**: 24521-24528; 1998.
11. Batinic-Haberle, I., Spasojevic, I., Hambright, P., Benov, L., Crumbliss, A. L. Fridovich, I., The relationship among redox potentials, proton dissociation constants of pyrrolic nitrogens, and in vitro and in vivo superoxide dismutring activities of manganese(III) and iron(III) water-soluble porphyrins, *Inorg. Chem.* **38**: 4011-4022; 1998.
12. Kachadourian, R., Batinic-Haberle, I., Fridovich I., Syntheses and superoxide dismutase activities of partially (1-4) β-chlorinated derivatives of manganese(III)-*meso*-tetrakis(*N*-ethylpyridinium-2-yl)porphyrin, *Inorg. Chem.* **38**: 291-396, 1999.
13. Okado-Matsumoto, A.; Batinic-Haberle, I.; Fridovich, I. Complementation of SOD deficient *Escherichia coli* by manganese porphyrin mimics of superoxide dismutase, *Free Radic. Biol. Med.* **37**: 401-410; 2004.
14. Warner, D. S., Sheng, H., Batinic-Haberle, I., Oxidants, Antioxidants, and the Ischemic Brain, *J. Exp. Biology*, **207**: 3221-3231; 2004.
15. Sheng, H, Wang, H, Homi, H. M., Spasojevic, I., Batinic-Haberle, I., Pearlstein, R. D., Warner, D. S., A No Laminectomy Spinal cord Compression Injury Model in Mice, *J. Neurotrauma*, **21**: 595-603; 2004.
16. Sheng, H., Enghild, J., Bowler, R., Patel, M., Calvi, C. L., Batinic-Haberle, I., Day, B. J., Pearlstein, R. D., Crapo, J. D., Warner, D. S., Effects of Metalloporphyrin Catalytic Antioxidants in Experimental Brain Ischemia, *Free. Radic. Biol. Med.*, **33**: 947-961; 2002.
17. Vujaskovic, Z., Batinic-Haberle, I., Rabbani, Z. N., Feng, Q.-F., Kang, S. K., Spasojevic, I., Samulski, T. V., Fridovich, I., Dewhirst, M. W., Anscher, M. S., A Small Molecular Weight Catalytic Metalloporphyrin Antioxidant with Superoxide Dismutase (SOD) Mimetic Properties Protects Lungs from Radiation-Induced Injury, *Free. Radic. Biol. Med.* **33**: 857-863; 2002.

18. Trostchansky, A., Ferrer-Sueta, G., Batthyany, C., Botti, H., Batinic-Haberle, I., Radi, R., Rubbo, H. Peroxynitrite-mediated LDL oxidation is inhibited by manganese porphyrins in the presence of uric acid, *Free Radic. Biol. Med.*, **35**: 1293-1300; 2003.
19. Piganelli, J. D., Flores, S. C., Cruz, C., Koepp, J., Young, R., Bradley, B., Kachadourian, R., Batinic-Haberle, I., Haskins, K., A., Metalloporphyrin Superoxide Dismutase Mimetic (SOD Mimetic) Inhibits Autoimune Diabetes, *Diabetes*, **51**: 347-355; 2002.
20. Aslan, M., Ryan, T. M., Adler, B., Townes, T. M., Parks, D. A., Thompson, J. A., Tousson, A., Gladwin, M. T., Tarpey, M., M., Patel, R. P., Batinic-Haberle, I., White, C. R., Freeman, B. A., Oxygen Radical Inhibition of Nitric-Oxide Dependent Vascular Function in Sickle Cell Disease, *Proc. Natl. Acad. Sci. USA*, **98**: 15215-15220; 2001.
21. Moeller, B. J., Batinic-Haberle, I., Spasojevic, I., Rabbani, Z. N., Anscher, M. S.; Vujaskovic, Z., Dewhirst, M. W., Effects of a catalytic metalloporphyrin antioxidant on tumor radioresponsiveness, *Int. J. Rad. Oncol. Biol. Phys.*, Submitted. 2004.
22. Sheng, H., Batinic-Haberle, I., Spasojevic, I., Friodvich, I., Warner, D. S., Mn(III) tetrakis(ortho N-ethylpyridyl)porphyrin, MnTE-2-PyP^{5+} (AEOL-10113) offers protection in mouse model of spinal cord injury, *Free Radic. Biol. Med.* **33**: S436: 2002.
23. Ferrer-Sueta, G., Batinic-Haberle, I., Spasojevic, I., Fridovich, I., Radi, R.,Catalytic scavenging of peroxynitrite by isomeric Mn(III) *N*-methylpyridylporphyrins in the presence of reductants, *Chem. Res. Toxicol.* **12**: 442-449; 1999.
24. Ferrer-Sueta, G.; Quijano, C.; Alvarez, B.; Radi, R. Reactions of manganese porphyrins and manganese-superoxide dismutase with peroxynitrite, *Methods Enzymol.* **349**: 23-39; 2002.
25. Ferrer-Sueta, G.; Vitturi, D.; Batinic-Haberle, I.; Fridovich, I.; Goldstein S.; Czapski, G.; Radi, R. Reactions of manganese porphyrins with peroxynitrite and carbonate radical anion, *J. Biol. Chem.* **278**: 27432-27438, 2003.
26. Batinic-Haberle, I., Spasojevic, I., Fridovich, I., Tetrahydrobiopterin Rapidly Reduces SOD Mimic, Mn(III) tetrakis(N-ethylpyridinium-2-yl)porphyrin, *Free Radic. Biol. Med.* **37**: 367-374; 2004.
27. Lukiw, W. J., Ottlecz, A., Lambrou, G., Grueninger, M., Finley, J., Thompson, H. W., Bazan, N, G., Coordinate activation of HIF-1 and NF-kB DNA binding and COX-2 and VEGF expression in retinal cells by hypoxia, *Invest. Ophtalomol. Vis. Sci.* **44**: 4164-4170; 2003.
28. Goyal, P., Weissmann, N., Grimminger, F., Hegel, C., Bader, L., Rose, F., Fink, L., Ghofrani, A. H., Schermuly, R. T., Schmidt, H.H. H. Seeger, W., Hanze, J., Upregulation of NAD(P)H oxidase 1 in hypoxia activates hypoxia-inducible factor 1 via increase in reactive oxygen species, *Free Radic. Biol. Med.* **36**: 1279-1288; 2004.
29. Sander, C. S., Chang, H., Hamm, F., Elsner, P., Thiele, J., J., Role of oxidative stress and the antioxidant network in cutaneous carcinogenesis, *Int. J. Dermatol.* **43**: 326-335; 2004.

30. Catani, M. V., Savini, I., Duranti, G., Caporossi, D., Ceci, R., Sabatini, S., Avigliano L., Nuclear factor kB and activating protein 1 are involved in differentiation-related resistance to oxidative stress in skeletal muscle cells, *Free Radic. Biol. Med.* **37**: 1024-1036; 2004.
31. Tse, H., Milton, M. J., Piganelli, J. D. Mechanistic analysis of the immunomodulatory effects of a catalytic antioxidant on antigen-presenting cells: Implication for their use in targeting oxidation/reduction reactions in innate immunity, *Free Radic. Biol. Med.* **36**: 233-247; 2004.
32. Zhao, Y., Chaiswing, L., Oberley, T. D., Batinic-Haberle, I., St. Clair, W., Epstein, C. J., St. Clair, D., A mechanism-based antioxidant approach for the reduction of skin carcinogenesis, *Cancer Res.*, 2004, submitted.
33. Moeller, B. J., Batinic-Haberle, I., Spasojevic, I., Rabbani, Z. N., Anscher, M. S., Vujaskovic, Z., Dewhirst, M. W. Effects of a catalytic metalloporphyrin antioxidant on tumor radioresponsiveness, *Int. J. Rad. Oncol. Biol. Phys.* 2004, Submitted.
34. (a) Moeller, B. J., Cao, Y., Li, Y. C., Dewhirst, M. W., Radiation activates HIF-1 to regulate vascular radiosensitivity in tumors: Role of oxygenation, free radicals, and stress granules, *Cancer Cell* **5**: 429-441; 2004; Moeller, B. J., Dewhirst, M. W., Raising the bar: How HIF-1 helps determine tumor radiosenstivity, *Cell Cycle*, 3; 2004 (published on line).
35. Vasquez-Vivar, J., Martasek, P., Whitsett, J., Joseph, J., Kalyanaraman, B., The ratio between tetrahydrobiopterin and oxidized tetrahydrobiopterin analogues controls superoxide release from endothelial nitric oxide synthase: an EPR trapping study, *Biochem. J.* **362**: 733-739; 2002.
36. Kinoshita, H., Tsutsui, M., Milstien, S., Katusic, Z. S., Tetrahydrobiopterin, nitric oxide and regulation of cerebral arterial tone, *Prog. Neurobiol.* **52**: 295-302; 1997.
37. Vasquez-Vivar, J., Hogg, N., Martasek, P., Karoui, H., Pritchard, Jr. K. A., Kalyanaramn, B., Tetrahydrobiopterin-dependent inhibition of superoxide generation from neuronal nitric oxide synthase, *J. Biol. Chem.* **274**: 26736-26742; 1999.
38. Vasquez-Vivar, J., Whitsett, J., Martasek, P., Hogg, N., Kalyanaram, B., Reaction of tetrahydrobiopterin with superoxide: EPR-kinetic analysis and characterization of the pteridine radical, *Free Radic. Biol. Med.* **31**: 975-985; 2001.
39. (a) Jones, C. L., Vasquez-Vivar, J., Griscavage, J., Masters, B. S. S., Martasek, P., Kalyanaraman, B. Gross, S. S., Only fully reduced pterins attenuate superoxide production by eNOS: an explanation for the tetrahydrobiopterin requirement? In Moncada. S., Gustafsson, L., Wiklund, P., Higgs, E. A., eds. *Biology of Nitric Oxide*, part 7. London: Portland Press; 2000, 118. (b) Raman, C. S., Martasek, P. Masters, B. S. S., Structural themes determining function in nitric oxide synthases, in Kadish, K. M., Smith, K. M., Guliard, R., eds., *The Porphyrin Handbook*, Vol. 4, Academic Press **2000**, 313-318.
40. (a) Hofseth, L. J., Hussain, S. P., Wogan, G. N., Harris, C. C., Nitric oxide in cancer and chemoprevention. *Free Rad. Biol. Med.* **34**: 955-968; 2003. (b) Thomsen, L. L., Miles, D. W., Role of nitric oxide in tumor progression: Lessons from human tumor, *Cancer Metastasis Rev.* **17**: 107-11; 1998.

41. Maulik, N., Das, D. K., Redox signaling in vascular angiogenesis, *Free Radic. Biol. Med.* **33**: 1047-1060; 2002.
42. Dulak. J., Jozkowicz, A., Dembinska-Kiec, A., Guevara, I., Zdzienicka, A., Zmudzinska-Grochot, D., Florek, I., Wojtowicz, A., Szuba, A., Cooke, J. P.,Nitric oxide induces the synthesis of vascular endothelial growth factor by rat vascular smooth muscle cells, *Arterioscler. Thromb. Vasc. Biol.* **20**: 659-666; 2000.
43. Ziche, M., Morbidelli, L., Choudhuri, R., Zhang, H.-T., Donnini, S., Granger, H. J., Bicknell, R., Nitric oxide synthase lies downstream from vascular endothelial growth factor-induced but not basic fibroblast growth factor-induced angiogenesis, *J. Clin. Invest.* **99**:2625-2634; 1997.
44. Shimizu, S., Yasuda, M., Ishii, M., Nagai, T., Kiuchi, Y., Yamamoto, T., Stimulation of in vitro angiogenesis by tetrahydrobiopterin in bovine aortic endothelial cells. *Jpn. J. Pharmacol.* **80**: 177-180; 1999.
45. Sun, Y. Free radicals, antioxidant enzymes, and carcinogensis, *Free Radic. Biol. Med.* **8**: 583-599; 1990.
46. Dabrowska-Ufniarz, E., Dzieniszewski, J., Jarosz, M., Wartanowicz, M., Vitamin C concentration in gastric juice in patients with precancerous lesions of the stomach and gastric cancer, *Med. Sci. Monit.* **8**: CR96-103; 2002.
47. Kumaraguruparan, R., Subapriya, R., Kabalimoorthy, J., Nagini, S., Antioxidant profile in the circulation of patients with fibroadenoma and adenocarcinoma of the breast, *Clin. Biochem.* **35**: 275-279; 2002.
48. Bozkir. A., Simsek. B., Gungor, A., Torun, M., Ascorbic acid and uric acid levels in lung cancer patients, *J. Clin. Pharmacol. Therap.* **24**: 43-47; 1999.
49. Abiaka, C., Al-Awadi, F., Gulshan, S., Al-Sayer, H., Behbehani, A., Farghaly, M., Simbeye, A., Plasma concentrations of alpha-tocopherol and urate in patients with different types of cancer, *J. Clin. Pharm. Therap.* **26**: 265-270; 2001.
50. (a) Jaruga, P., Zastawny, T. H., Skokowski J., Dizdaroglu, M., Olinski, R., Oxidative DNA base damage and antioxidant enzyme activities in human lung cancer. *FEBS Lett.* **341**: 59-64; 1994; (b) Kinnnula, V. L., Crapo, J. D. Superoxide dismutases in malignant cells and tumors, *Free Radic. Biol. Med.* 36: 718-744; 2004.
51. Patel, K. B., Stratford, M. R. L., Wardman, P., Everett, S. A., Oxidation of tetrahydrobiopterin by biological radicals and scavenging of the tetrahydrobiopterin radical by ascorbate, *Free Radic. Biol. Med.* **32**: 203-211; 2002.
52. Kokolis, N., Ziegler, I., On the levels of phenylalanine, tyrosine and tetrahydrobiopterin in the blood of tumor-bearing organism, *Cancer Biochem. Biophys.* **2**: 79-85; 1977.
53. Shang, T., Kotamraju, S., Kalivendi, S. V., Hillard, C. J., Kalyanaraman, B., 1-Methyl-4-phenylpyridinium-induced apoptosis in cerebellar granule neurons is mediated by transferrin receptor iron-dependent depletion of tetrahydrobiopterin and neuronal nitric oxide synthase-derived superoxide, *J. Biol. Chem* .279: 19099-19112; 2004.
54. Spasojevic, I., Batinic-Haberle, I., Fridovich, I., Nitrosylation of manganese(III) tetrakis(N-ethylpyridinium-2-yl)porphyrin: A simple and sensitive

spectrophotometric assay for nitric oxide, *Nitric Oxide: Biol. Chem.* **4**: 526-533; 2000.
55. Gorren, A. C. F., Kungl, A. J., Schmidt, K., Werner, E. R., Mayer, B., Electrochemistry of pterin cofactors and inhibitors of nitric oxide synthase, *Nitric Oxide: Biol. Chem.* **5**: 176-186; 2001.
56. Archer, M. C., Vonderschmitt, D. J., Scrimgeour, K. G., Mechanism of oxidation of tetrahydrobiopterins, *Can. J. Biochem.* **50**: 1174-1182; 1972.
57. Fukushima, T., Nixon, J. C., Analysis of reduced forms of biopterin in biological tissues and fluids, *Anal. Biochem.* **102**: 176-188; 1990.
58. Fiege, B., Ballhausen, D., Kierat, L., Leimbacher, W., Goriounov, D., Schircks, B., Thony, B., Blau, N., Plasma tetrahydrobiopterin and its pharmacokinetic following oral administration, *Mol. Genet. Metab.* **81**: 45-51; 2004.
59. Meininger, C. J., Wu, G., Regulation of endothelial cell proliferation by nitric oxide, *Methods Enzymol.* **352**: 281-292; 2002.
60. Milstein, S., Katusic, Z., Oxidation of tetrahydrobiopterin by peroxynitrite: Implications for vascular endothelial function, *Biochem. Biophys. Res. Commun.* **263**: 681-684; 1999.
61. Davis, M. D., Kaufman, S., Milstein, S., The auto-oxidation of tetrahydrobiopterin, *Eur. J. Biochem.* 173: 345-351; 1988.
62. Archer, M. C., Schrimgeour, K. G., Rearrangement of quinoid dihydropteridines to 7,8-dihydropteridines, *Can. J. Biochem.* 48: 278-287; 1970.
63. Archer, M. C., Vonderschmidt, D. J., Scrimgeour, K. G., Mechansim of oxidation of tetrahydropterins, *Can. J. Biochem.* 50: 1174-1182; 1972.
64. Armarego, W. L. F., Randles, D., Taguchi, H., Peroxidase catalysed aerobic degradation of 5,6,7,8-tetrahydrobiopterin at physiological pH, *Eur. J. Biochem.* **135**: 393-403; 1983.
65. Kruse, A., Broholm, H., Rubin, I., Schmidt, K., Lauritzen, M., Nitric oxide synthase activity in human pituitary adenomas, *Acta Neurol. Scand.* **106**: 361-366; 2002.
66. Ziche, M., Morbidelli, L., Determinaion of Angiogenesis-relating oproperties of NO, *Methods Enzymol.* **352**: 407-421; 2002.
67. Bredt, D. S., Schmidt, H. H. H. W., The citrulline assay, in *Methods in Nitric Oxide Research*, 249-255;1996.
68. Fujii J. Nitric oxide synthase (NOS) activity assay: RI method to detect L-citruline. In *Experimental protocols for reactive oxygen and nitrogen species*, eds. Taniguchi N, Gutteridge JMC, Oxford University Press, 1999.
69. Dewhirst, M. W., Oliver, R., Tso, C. Y., Gustafson, C., Secomb, T., Gross, J. F., Heterogeneity in tumor microvascular response to radiation, *Int. J. Rad. Oncol. Biol. Phys.***18**: 559-568; 1990.
70. Shan, S., Sorg, B., Dewhirst, M. W., A novel rodent mammary window of orthotopic breast cancer for intravital microscopy, *Microvasc. Res.* **65**: 109-117; 2003.

APPENDICES

2. *Free Radic. Biol. Med.* **37**: 367-374; 2004

Tetrahydrobiopterin Rapidly Reduces the SOD Mimic, Mn(III) *Ortho* Tetrakis (*N*-ethylpyridinium-2-yl)porphyrin

By

Ines Batinic-Haberle[1*] Ivan Spasojevic[2], Irwin Fridovich[3]
Departments of Radiation Oncology,[1] Medicine,[2] and Biochemistry[3], Duke University Medical Center, Durham, NC 27710

Running title: *Tetrahydrobiopterin reduces SOD mimic*

Key words: SOD mimics, NO, nitric oxide synthase, tumor anti-angiogenesis, Mn(III) tetrakis(*N*-ethylpyridinium-2-yl)porphyrin and Mn(III) tetrakis(*N*-n-octylpyridinium-2-yl)porphyrin, tetrahydrobiopterin, 7,8-dihydrobiopterin, L-sepiapterin,

*corresponding author:
Tel: 919-684-2101
Fax: 919-684-8885
e-mail: ibatinic@duke.edu

Summary

Mn(III) *ortho* tetrakis(*N*-ethylpyridinium-2-yl)porphyrin, Mn^{III}TE-2-PyP^{5+}, effectively scavenges reactive oxygen and nitrogen species *in vitro,* and protects *in vivo,* in different rodent models of oxidative stress injuries. Further, Mn^{III}TE-2-PyP^{5+} was shown to be readily reduced by cellular reductants such as ascorbic acid and glutathione. We now show that tetrahydrobiopterin (BH_4) is also able to reduce the metal center. Under anaerobic conditions, in phosphate-buffered saline (pH 7.4) at 25 $\pm$ 0.1 ^{0}C, reduction of Mn^{III}TE-2-PyP^{5+} occurs through two reaction steps with rate constants $k_1 = 1.0 \times 10^4$ M^{-1} s^{-1} and $k_2 = 1.5 \times 10^3$ M^{-1} s^{-1}. We ascribe these steps to the formation of tetrahydrobiopterin radical ($BH_4^{\cdot+}$) (k_1) that than undergoes oxidation to 6,7-dihydro-8*H*-biopterin (k_2), which upon rearrangement gives rise to 7,8-dihydrobiopterin (7,8-BH_2). Under aerobic conditions, Mn^{III}TE-2-PyP^{5+} catalytically oxidizes BH_4. This is also true for its longer-chain alkyl analogue, Mn(III) tetrakis(*N*-n-octylpyridinium-2-yl)porphyrin. The reduced Mn(II) porphyrin cannot be oxidized by 7,8-BH_2 or by L-sepiapterin. The data are discussed with regards to the possible impact of the interaction of Mn^{III}TE-2-PyP^{5+} with BH_4 on endothelial cell proliferation and hence on tumor anti-angiogenesis *via* inhibition of nitric oxide synthase.

Introduction

Mn(III) *ortho* 5,10,15,20-tetrakis(*N*-ethylpyridinium-2-yl)porphyrin, Mn^{III}TE-2-PyP^{5+} (Scheme I) [1] protects versus several rodent models of oxidative stress, such as cancer/radiation [2], stroke [3], diabetes [4], and sickle cell disease [5]. Its protective effects have been ascribed to its antioxidant properties [6-9]. *In vitro* it catalyzes the dismutation of $O_2^{\cdot-}$ with rate constant of 5.7×10^7 M^{-1} s^{-1} [6,7]. In addition it was found reactive at comparable or higher rates towards $ONOO^-$, $ONOOCO_2^-$, $^{\cdot}NO$, and $CO_3^{\cdot-}$ [1,8,9,10]. Tissue localization of Mn porphyrins and local concentrations of reactive oxygen (ROS) and nitrogen species (RNS) would define which reaction predominates in the overall effects observed *in vivo*.

Manganese in Mn porphyrins can access four oxidation states, +2, +3, +4 and +5 [1]. *In vitro* , most Mn porphyrins are stable when Mn is in its +3 oxidation state [1]. However, the Mn(III) *N*-alkylpyridylporphyrins are readily reducible. The redox potential for $Mn^{III}P^{5+}/Mn^{II}P^{4+}$ redox couple is +0.23 V *vs* NHE for ethyl, MnTE-2-PyP^{5+} [1] and +0.37 V *vs* NHE for its longer alkyl chain analogue, the n-octyl compound, Mn^{III}TnOct-2-PyP^{5+} (Scheme I) [11]. Consequently, the manganese undergoes reduction from +3 to +2 oxidation state *in vivo* (*E. coli*) [6] and *in vitro* [10-13][a] by cellular reductants, such as ascorbic acid and glutathione. When Mn(III) or Mn(II) porphyrins scavenge $ONOO^-$, H_2O_2 and $CO_3^{\cdot-}$, the $O{=}Mn^{IV}P^{4+}$ is formed [1,8,9] and is readily reduced by uric acid, ascorbic acid, and glutathione with rate constants of 3.5×10^7 M^{-1} s^{-1}, 4×10^4 M^{-1} s^{-1}, and 1.22×10^6 M^{-1} s^{-1}, respectively [8]. The reduction of either $Mn^{III}P^{5+}$ or $O{=}Mn^{IV}P^{4+}$ by cellular reductants appears essential for the beneficial effect of Mn(III) porphyrins, and for assuring the catalytic nature of their action [8,9,12,14,15]. Moreover, the reduced Mn(II) porphyrins react with $O_2^{\cdot-}$ and $CO_3^{\cdot-}$ faster than their Mn(III) analogues [7,9]. Preliminary data [9] indicate that the reaction of Mn(II) porphyrins with $ONOO^-$ is also fast, and the two-electron oxidation of the Mn^{+2} by $ONOO^-$ produces nitrite rather than $^{\cdot}NO_2$ radical. The latter is formed when Mn(III) porphyrin gets oxidized by $ONOO^-$ [8,9].

In addition to scavenging ROS and RNS, Mn porphyrins were found to affect signaling processes [4,16-19]. The anionic porphyrin, $MnTCPP^{3-}$ ($MnTBAP^{3-}$) has been implicated in induction of hemeoxygenase-1 [16]. Tse et al reported that the cationic porphyrins, Mn^{III}TE-2-PyP^{5+} and Mn(III) tetrakis(*N,N'*-diethylimidazolium-2-yl)porphyrin, Mn^{III}TDE-2-ImP^{5+} oxidize a cysteine of the p50 subunit of transcription factor NF-κB, therefore decreasing NF-κB binding to DNA and diminishing proinflammatory cytokine and ROS production [18]. The ability to oxidize a p50 cysteine is consistent with the ability of Mn^{III}TE-2-PyP^{5+} to oxidize glutathione [13].[a] Also, Zhoung et al reported that Mn^{III}TE-2-PyP^{5+} decreases the DNA binding ability of AP-1 transcription factor; that action was thought to be relevant to carcinogenesis [19]. Whatever mechanism/s of action of Mn^{III}TE-2-PyP^{5+} is operative *in vivo*, the modulation of cellular redox systems and consequently cell proliferation, apoptosis and angiogenesis is likely to be involved. Thorough knowledge of the complex reactivity of Mn porphyrins intended for the treatment of oxidative stress injuries is essential for understanding their effects.

We have recently observed that MnTE-2-PyP^{5+} exerts tumor anti-angiogenic effects in mice when administered intraperitoneally [20]. Due to the recognized role of $^{\cdot}NO$ in angiogenesis [21,22], and the favorable anti-tumor effects observed with inducible iNOS inhibitors [21], we were interested in exploring whether the nitric oxide-related chemistry of Mn porphyrins may be involved in their anti-tumor action. We have already reported that MnTE-2-PyP^{5+} could be reductively nitrosylated [10]. Yet, this reaction is stoichiometric and under low oxygen concentration fairly irreversible and is not likely to significantly decrease steady state $^{\cdot}NO$ levels *in vivo* [10]. In this study, we explored the catalytic oxidation of tetrahydrobiopterin (BH_4) (Scheme II), the cofactor of nitric oxide synthase (NOS) [23,24], by Mn porphyrins, which could affect steady state $^{\cdot}NO$ levels. We compared ethyl porphyrin to its longer-alkyl chain analogue, n-octyl porphyrin Mn^{III}TnOct-2-PyP^{5+} [11] (Scheme I), in order to see whether differences in the sterics and solvation of these porphyrins may affect their interactions with BH_4. Since n-octyl porphyrin is 6-fold more lipophilic, it localizes inside *E. coli* more than does ethyl compound, offering 30-fold higher protection [25]. Therefore, given similar reactivities, we anticipate that MnTnOct-2-PyP^{5+} may potentially be a better anti-tumor drug than MnTE-2-PyP^{5+}, since it could more readily localize inside tumor and be more suitable for liposome-directed delivery.

Experimental

Materials. Mn^{III}TE-2-PyP^{5+} and Mn^{III}TnOct-2-PyP^{5+} were synthesized as previously described [1,11]. The (6R)–5,6,7,8-tetrahydro-L-biopterin dihydrochloride, 7,8-dihydro-L-biopterin and L-

sepiapterin are purchased from Alexis Biochemicals. L-ascorbic acid (+99 %) was from Aldrich. The phosphate-buffered saline (PBS) was from GIBCO.

Methods. ***Uv/vis spectrometry.*** A Shimadzu UV-2501PC was used for uv/vis spectral measurements. In the first experiment, 1 mM aqueous solutions of Mn^{III}TE-2-PyP^{5+} and M^{III}TnOct-2-PyP^{5+} were diluted to 5 and 3 μM, respectively, into PBS, argon purged for 15 min, followed by the addition of 0.3 mM BH_4 solution. In a second experiment the reactivity of reduced Mn^{II}TE-2-PyP^{4+} with oxidized pterins was studied. Thus, the Mn^{III}TE-2-PyP^{4+} was diluted up to 5 or 6 μM into PBS, argon purged 15 min, ascorbic acid added to 12 μM followed by the addition of 7,8 BH_2 or L-sepiapterin up to 0.4 mM or 0.3 mM, respectively. All stock solutions were purged with argon before dilution when anaerobic conditions were intended.

Oxygen consumption. Oxygen consumption was measured with a Clark electrode as previously described [10]. In the first experiment, the air-equilibrated PBS (V_{tot} = 2.4 mL) was first treated with 0.21 mg (0.35 mM) BH_4 followed by the addition of 5 μM Mn(III) porphyrin. In a second experiment, the air-equilibrated PBS (V_{tot} = 2.4 mL) was first treated with 5 μM Mn (III) porphyrin, followed by the addition of 0.9 mM BH_4. Finally, $Na_2S_2O_4$ was added to establish anaerobic baseline.

Stopped-flow kinetics. Kinetics were carried out on an Applied Photophysics stopped-flow instrument at 25 ± 0.1°C and pH 7.4 (PBS) under anaerobic conditions. 12 μM Mn^{III}TE-2-PyP^{5+} and 60 μM to 1.2 mM BH_4 were prepared and purged with argon before mixing in 1 : 1 ratio. The reduction of Mn^{III}TE-2-PyP^{5+} was followed spectrally as disappearance of the Soret band at 454 nm (1).

Results

Uv/vis spectrometry. Both aerobically and anaerobically Mn^{III}TE-2-PyP^{5+} and Mn^{III}TnOct-2-PyP^{5+} were reduced by BH_4 (Figure 1A). The Soret bands of Mn^{II}TE-2-PyP^{4+} and Mn^{II}TnOct-2-PyP^{4+} were centered at 438.5 nm and 441.5 nm, respectively. A shift in wavelength from 454 nm to 438.5 nm was previously observed when Mn^{III}TE-2-PyP was reduced with either ascorbic acid or glutathione [10,13],[a] indicating that identical species were formed upon reduction with either reductant. Uv/vis measurements indicated that Mn(II) porphyrins, reduced with ascorbic acid, were not reoxidized by the oxidized pterins, 7,8-BH_2 (Figure 1B) and L-sepiapterin (Figure 1B-inset). With 7,8-BH_2 no shift in Soret band was observed (Figure 1B). In the case of L-sepiapterin due to its high absorption in the Soret region, the lack of shift at porphyrin 566 nm band indicated that no oxidation of Mn(II) porphyrin occurred (Figure 1B-inset). Ascorbic acid itself was reported not to react with 7,8-BH_2 [23], and thus did not interfere with these measurements. Sepiapterin is not likely to be reduced by ascorbic acid either since no reduction by cyclic voltammetry up to -820 mV was reported by Gorren et al [26]. The same authors reported the lack of a reduction wave for 7,8-BH_2 below -1.0 V [26].

Oxygen consumption. A slow oxygen consumption due to auto-oxidation of BH_4 was detected as shown in Figure 2. When Mn(III) porphyrin and BH_4 were both present in solution, oxygen consumption was greatly enhanced, indicating that Mn(III) porphyrin catalyzes the oxidation of BH_4 (Figure 2). The efficiency of this catalysis was similar with both MnTE-2-PyP^{4+} and MnTnOct-2-PyP^{4+} (Figure 2, solid and dotted lines).

Stopped-flow kinetics. Two reaction steps were observed, each comprising ~50% drop in absorbance of MnTE-2-PyP^{5+}. The observed pseudo-first order rate constants, k_{obs}, of both reactions were linearly dependent upon BH_4 concentration (Figure 3). From the plots k_{obs} *vs* [BH_4] the second order rate constants, k_1 and k_2 were calculated to be $k_1 = 1.0 \times 10^4\ M^{-1}\ s^{-1}$ and $k_2 = 1.5 \times 10^3\ M^{-1}\ s^{-1}$.

Discussion

The *in vivo* efficacy of the catalytic antioxidant Mn^{III}TE-2-PyP^{5+} has been mostly ascribed to its ability to scavenge reactive oxygen and nitrogen species [1,6-11]. New data indicate that other actions *in vivo* (see Introduction) may be effective [18,19]. This study was undertaken in order to gain insights into the additional actions of Mn^{III}TE-2-PyP^{5+} and its analogues in biological systems, particularly those related to anti-tumor effects.

Because of the high metal-centered redox potential for Mn^{III}/Mn^{II} redox couple ($E_{1/2}$=+230 mV *vs* NHE), Mn^{III}TE-2-PyP^{5+} undergoes reduction by cellular reductants [10,13][a]. The reduction with ascorbic acid is facile, presumably utilizing $A^{2-}/A^{\cdot-}$ redox couple (E° = +19 mV *vs* NHE, pK_a (HA^{-}/A^{2-},H^{+}) = 11.34) [11,27]. The reaction of Mn^{III}TE-2-PyP^{5+} with glutathione [27] is significantly slower. At 6 μM Mn^{III}TE-2-$PyP^{5+}$and 606 μM GSH, under anaerobic conditions, 50% of the porphyrin was reduced in 5 min.[a]

Aerobically, at 100-fold excess of GSH, and at pH 7.4 (PBS), only negligible reduction of Mn^{III}TE-2-PyP^{5+} occurred.[a] When in addition to GSH, nitric oxide was present the reductive nitrosylation occurred readily.[a] This is so because binding of nitric oxide shifts the effective potential for the Mn^{III}/Mn^{II} redox couple of a porphyrin by ~ + 600 mV [29-31] and is a driving force for Mn^{III}P reduction. While uric acid ($E_{1/2}$ for $UA/UA^{\cdot}$ = +590 mV *vs* NHE) [32] itself can not reduce Mn^{III}TE-2-PyP^{5+} [14],[a] in the presence of $^{\cdot}NO$ reductive nitrosylation occurred readily.[a]

We have shown here that tetrahydrobiopterin readily reduces Mn^{III}TE-2-PyP^{5+}, giving rise to Mn^{II}TE-2-PyP^{4+}. Based on cyclic voltammetry, Gorren et al [26] reported that one-electron oxidation of tetrahydrobiopterin, BH_4 (as well as of tetrahydropterin) to $BH_4^{\cdot+}$ (at N 5, Scheme II) occurs at +270 mV *vs* NHE (pH 7.0). Using polarography, Archer et al [33] reported that reduced pterin (tetrahydropterin) undergoes reversible oxidation by two overlapping one-electron steps at +150 mV vs NHE (pH 7.0) producing 6,7-BH_2, which upon rearrangement gives rise to 7,8-BH_2. The authors [33] coupled the oxidation of pterin to the $Fe^{III}(CN)_6^{3-}/Fe^{II}(CN)_6^{4-}$ redox couple (E°= + 358 mV *vs* NHE), whose reduction potential is similar to the potentials of Mn(III) porphyrins studied (+228 and +367 mV *vs* NHE for ethyl and n-octyl porphyrin, respectively, ref 11). In both studies, 7,8-BH_2 is the ultimate product of BH_4 oxidation. Based on the data reported [26,33], the two-step reduction of Mn^{III}TE-2-PyP^{5+} with tetrahydrobiopterin presumably occurs through eqs [1] and [2]:

$$BH_4 + Mn^{III}T(alkyl)\text{-}2\text{-}PyP^{5+} \Longleftrightarrow BH_4^{\cdot+} + Mn^{II}T(alkyl)\text{-}2\text{-}PyP^{4+} \quad k_1 \quad [1]$$

$$BH_4^{\cdot+} + Mn^{III}T(alkyl)\text{-}2\text{-}PyP^{5+} \Longleftrightarrow 6,7\text{-}(8H)\text{-}BH_2 + Mn^{II}T(alkyl)\text{-}2\text{-}PyP^{4+} + 2H^{+} \quad k_2 \quad [2]$$

$$6,7\text{-}(8H)\text{-}BH_2 \Longleftrightarrow 7,8\text{-}BH_2 \quad [3]$$

We ascribed the k_1 (1.0×10^4 M^{-1} s^{-1}) to one-electron oxidation of BH_4 to $BH_4^{\cdot+}$ radical (eq 1), and k_2 (1.5×10^3 M^{-1} s^{-1}) to the one electron oxidation of $BH_4^{\cdot+}$ to 6,7-(8*H*)-BH_2 (eq 2). As was the case with ascorbic acid, glutathione and uric acid, reductive nitrosylation of Mn^{III}TE-2-PyP^{5+} occurs readily in the presence of both BH_4 and $^{\cdot}NO$.[a]

In addition to their identical reactivities towards $O_2^{\cdot-}$, $ONOO^{-}$ and $CO_3^{\cdot-}$ [9,11] both Mn^{III}TE-2-PyP^{4+} and Mn^{III}TnOct-2-PyP^{4+} oxidize tetrahydrobiopterin (Figure 1) in a catalytic manner aerobically, and at similar rates (Figure 2). In a first step of a catalytic cycle both porphyrins got reduced by BH_4 and may be reoxidized in a second step of a catalytic cycle with either oxygen or any ROS such as $O_2^{\cdot-}$, or $ONOO^{-}$, or $CO_3^{\cdot-}$. However, *in vivo* their behavior is quite different presumably due to the differences in bulkiness and lipophilicity [11,25]. Our *E. coli* study showed that the n-octyl porphyrin localized within the cell significantly more than ethyl compound due to its higher lipophilicity, and was thus more protective to SOD-deficient strain at 30-fold lower concentration [25]. Further, MnTE-2-PyP^{5+} decreased blood pressure in rats [34], while MnTnOct-2-PyP did not,[b] when both compound were given intravenously. Given their identical reactivity towards $O_2^{\cdot-}$, preventing the elimination of $^{\cdot}NO$ through $ONOO^{-}$ formation is not likely in the origin of such an effect. The uncoupling of endothelial eNOS through depletion of BH_4 is not responsible for this effect either, since it would have resulted in the increase of blood pressure with both porphyrins.

Tetrahydrobiopterin is a co-factor of nitric oxide synthase [23,24], and hence is an indirect regulator of vascular tone. The BH_4 appears to be essential for driving the synthesis of L-citrulline and $^{\cdot}NO$ formation by preventing the dissociation of the heme-Fe(II) dioxygen/heme-Fe(III) superoxide complex (thereby preventing the formation of superoxide), and by promoting the generation of heme-Fe(III) peroxo and heme-Fe(IV) oxo species [35]. Only fully reduced tetrahydrobiopterin (and not 7,8-BH_2) can support NOS catalysis [36,37]. Several *in vitro* studies directly established the role of $^{\cdot}NO$ and BH_4 in angiogenesis [21,22,38-40].

Tumor tissue is under persistent oxidative stress with balance between cell proliferation and cell death shifted inappropriately toward excess proliferation, and with levels of antioxidants altered [41]. Both decreased and increased levels of superoxide dismutases, lower levels of catalase and lower levels of low-molecular weight antioxidants, such as ascorbic acid, uric acid and vitamin E have been reported in tumors [41-46]. Oxidative stress also results in over-expression of iNOS [21], accompanied by BH_4 levels higher than are found in normal tissue [47,48]. Due to the positive correlation between iNOS activity and tumor progression, iNOS inhibitors have been tested for cancer therapy [21]. In the tumor environment Mn porphyrins - particularly the more lipophilic n-octyl compound since it would localize in a tumor to a higher degree than ethyl - may selectively affect the levels of particular reductants, like BH_4, whose micromolar cellular levels [47,48] are much more sensitive to fluctuations than are the mM levels of

glutathione and ascorbic acid. The catalytic depletion of BH_4 by either MnTE-2-PyP^{5+} or MnTnOct-2-PyP^{5+} would inhibit NO production by iNOS which in turn would impact signaling processes and angiogenesis. This could be a likely explanation for the tumor anti-angiogenic effects, followed by tumor shrinkage that we observed when mice bearing tumors were treated intraperitoneally with 6mg/kg/day of Mn^{III}TE-2-PyP^{5+} [20]. The depletion of BH_4 by H_2O_2-derived oxidized iron species (perferryl iron) in cerebellar granule neurons was observed by Kalyanaraman group [49], and it occurred presumably in a similar manner as with Mn(III) porphyrins. The BH_4 depletion resulted in production of $O_2^{\cdot-}$ by NOS rather than NO [49]. Testing the effect of Mn^{III}TE(nOct)-2-PyP^{5+} on tumor BH_4 depletion, and NOS inactivation is in progress.

Abbreviations: BH_4, (6R)–5,6,7,8-tetrahydro-L-biopterin; 6,7-BH_2, 6,7- dihydro-8*H*-biopterin; 7,8-BH_2, 7,8-dihydro-L-biopterin; L-sepiapterin, sep; ROS and RNS, reactive oxygen and nitrogen species; NO, nitric oxide; NOS; nitric oxide synthase; iNOS, inducible nitric oxide synthase; SOD, superoxide dismutase; AA, ascorbic acid; AN, acetonitrile; GSH, glutathione; UA, uric acid; NF-κB, nuclear factor κB; AP-1, activator protein-1; PBS, phosphate-buffered saline; $Mn^{III/II}P^{5+/4+}$, any Mn(III/II) *meso* tetrakis *N*-alkylpyridylporphyrin; *meso* refers to the substituents at the 5,10,15, and 20 (*meso* carbon) position of the porphyrin core; O=$Mn^{IV}P^{4+}$, any O=Mn(IV) *meso* tetrakis *N*-alkylpyridylporphyrin; Mn^{III}T(alkyl)-2-PyP^{5+}, alkyl E, ethyl; nOct, n-octyl on the pyridyl ring; 2 indicates that Mn porphyrin is an *ortho* isomer; Mn^{III}TE-2-PyP^{5+} is AEOL-10113, and Mn^{III}TDE-2-ImP^{5+} (Mn(III) 5,10,15,20-tetrakis(*N,N'*-diethylimidazolium-2-yl)porphyrin) is AEOL-10150; Mn^{III}TDE-2-ImP^{5+} has previously (ref 7 and elsewhere) been incorrectly abbreviated as MnTDE-1,3-ImP^{5+}, whereby 1 and 3 indicated the imidazolyl nitrogens, rather than the position 2 where the imidazolyl is attached to the porphyrin ring; $MnTCPP^{3-}$ ($MnTBAP^{3-}$), Mn(III) 5,10,15,20-tetrakis(4-carboxylatophenyl)porphyrin.

Acknowledgment: The authors appreciate helpful discussions with Gerardo Ferrer-Sueta and are thankful to Alvin L. Crumbliss for using his stopped-flow apparatus. The authors are also grateful for financial support from DOD CDMRP BC024326, Christopher Reeve Paralysis Foundation BA1-0103-1, Aeolus/Incara Pharmaceuticals, RTP, NC and the National Institute of Neurological Disorders and Stroke.

Footnotes:

[a] Batinic-Haberle, I.; Spasojevic, I. unpublished data.

[b] Spasojevic, I.; Calvi, C. L.; Batinic-Haberle, I.; Warner. D. unpublished data.

References

1. Batinic-Haberle, I.; Spasojevic, I.; Hambright, P.; Benov, L.; Crumbliss, A. L. Fridovich, I. The relationship among redox potentials, proton dissociation constants of pyrrolic nitrogens, and in vitro and in vivo superoxide dismutring activities of manganese(III) and iron(III) water-soluble porphyrins. *Inorg. Chem.* **38**: 4011-4022; 1998.
2. Vujaskovic, Z, Batinic-Haberle I, Rabbani ZN, Feng Q.-F, Kang SK, Spasojevic, I.; Samulski, T. V.; Fridovich, I.; Dewhirst, M. W.; Anscher, M. S. A small molecular weight catalytic metalloporphyrin antioxidant with superoxide dismutase (SOD) mimetic properties protects lungs from radiation-induced injury. *Free Radic. Biol. Med.* **33**: 857-863; 2002.
3. Sheng, H.; Enghild, J. J.; Bowler, R.; Patel, M.; Batinic-Haberle I.; Calvi, C. L.; Day, B. J.; Pearlstein, R. D.; Crapo, J. D.; Warner, D. S. Effects of metalloporphyrin catalytic antioxidants in experimental brain ischemia. *Free. Radic. Biol. Med.* **33:** 947-961; 2002.
4. Piganelli, J. D; Flores, S. C.; Cruz, C.; Koepp, J.; Batinic-Haberle, I.; Crapo, J.; Day, B; Kachadourian, R.; Young, R.; Bradley, B.; Haskins, K. Metalloporphyrin-based superoxide dismutase mimic inhibits adoptive transfer of autoimmune diabetes by a diabetogenic T-cell clone. *Diabetes* **51**: 347-355; 2002.
5. Aslan, M.; Ryan, T. M.; Adler B.; Townes, T. M.; Parks D. A.; Thompson, J. A.; Tousson, A.; Gladwin, M. T.; Patel, R. P.; Tarpey, M. M.; Batinic-Haberle, I.; White, C. R.; Freeman, B. A. Oxygen radical inhibition of nitric oxide-dependent vascular function in sickle-cell disease. *Proc. Natl. Acad. Sci. USA* **98**: 15215-15220, 2001.

6. Batinic-Haberle, I.; Benov, L.; Spasojevic, I.; Fridovich, I. The *ortho* effect makes manganese(III) meso-tetrakis(N-methylpyridinium-2-yl)porphyrin a powerful and potentially useful superoxide dismutase mimic. *J. Biol. Chem.* **273**: 24521-24528; 1998.
7. Spasojevic, I.; Batinic-Haberle, I.; Reboucas, J. S.; Idemori, Y. M.; Fridovich, I.; Electrostatic contribution in the catalysis of $O_2^{\cdot-}$ dismutation by superoxide dismutase mimics. $Mn^{III}TE\text{-}2\text{-}PyP^{5+}$ vs $MnBr_8T\text{-}2\text{-}PyP^{+}$. *J. Biol. Chem.* 278: 6831-6837; 2003.
8. Ferrer-Sueta, G.; Batinic-Haberle, I.; Spasojevic, I.; Fridovich, I.; Radi, R. Catalytic scavenging of peroxynitrite by isomeric Mn(III) *N*-methylpyridylporphyrins in the presence of reductants. *Chem. Res. Toxicol.* **12**: 442-449; 1999.
9. Ferrer-Sueta, G.; Vitturi, D.; Batinic-Haberle, I.; Fridovich, I.; Goldstein S.; Czapski, G.; Radi, R. Reactions of manganese porphyrins with peroxynitrite and carbonate radical anion. *J. Biol. Chem.* **278**, 27432-27438, 2003.
10. Spasojevic, I.; Batinic-Haberle, I.; Fridovich, I. Nitrosylation of manganese(III) tetrakis(N-ethylpyridinium-2-yl)porphyrin: A simple and sensitive spectrophotometric assay for nitric oxide. *Nitric Oxide: Biol. Chem.* **4**: 526-533; 2000.
11. Batinic-Haberle, I.; Spasojevic, I.; Stevens, R. D.; Hambright, P.; Fridovich, I. Manganese(III) *meso*-tetrakis(*ortho*-*N*-alkylpyridyl)porphyrins. Synthesis, characterization, and catalysis of $O_2^{\cdot-}$ dismutation. *J. Chem. Soc. Dalton Trans.* 2689-2696; 2002.
12. Bloodsworth, A.; O'Donnell, V. B.; Batinic-Haberle, I.; Chumley, P. H.; Day, B. J.; Crow, J. P.; Freeman, B. A. Manganese-porphyrin reactions with lipids and lipoproteins. *Free Radic. Biol. Med.* **28**: 1017-1029; 2000.
13. Pfeiffer, S.; Schrammel, A.; Koesling, D; Schmidt, K.; Meyer, B. Molecular actions of a Mn(III) porphyrin superoxide dismutase mimic and peroxynitrite scavenger: Reaction with nitric oxide and direct inhibition of NO synthase and soluble guanylyl cyclase. *Mol. Pharmacol.* **53**: 795-800; 1998.
14. Trostchansky, A., Ferrer-Sueta, G., Batthyany, C., Botti, H., Batinic-Haberle, I., Radi, R., Rubbo, H. Peroxynitrite-mediated LDL oxidation is inhibited by manganese porphyrins in the presence of uric acid. *Free Radic. Biol. Med.* **2003**, 35, 1293-1300.
15. Perez, M. J.; Cederbaum, A. I. Antioxidant and pro-oxidant effects of a manganese porphyrin complex against CYP2E1-dependent toxicity. *Free Radic. Biol. Med.* **33**: 111-127; 2002.
16. Konorev, E. A.; Kotamraju, S.; Zhao, H.; Kalivendi, S.; Joseph, J.; Kalyanaraman B. Paradoxical effects of metalloporphyrins on doxorubicin-induced apoptosis: Scavenging of reactive oxygen species versus induction of heme-oxygenase-1. *Free Radic. Biol. Med.* **33**: 988-997; 2002.
17. Bowler, R.; Sheng, H.; Enghild, J.; Duda, B.; Crapo, J. D.; Warner, D. S. A superoxide dismutase mimic attenuates changes in gene expression after stroke. *Free Radic. Biol. Med.* **33**: 1141-1152; 2002.
18. Tse, H., Milton, M. J., Piganelli, J. D. Mechanistic analysis of the immunomodulatory effects of a catalytic antioxidant on antigen-presenting cells: Implication for their use in targeting oxidation/reduction reactions in innate immunity. *Free Radic. Biol. Med.* **36**: 233-247; 2004.
19. Zhao, Y., Chaiswing, L., Oberley, T., Batinic-Haberle, I., Fridovich, I., Epstein, C., St. Clair, D. Mechanism based modulation of skin carcinogenesis by SOD mimetic in manganese superoxide dismutase deficiency mice. *Free Radic. Biol. Med.* **35** (Suppl. 1) S173-S173, 2003.
20. Moeller, B. J.; Batinic-Haberle, I.; Spasojevic, I.; Rabbani, Z. N.; Anscher, M. S.; Dewhirst, M. W.; Vujaskovic, Z. A Novel Superoxide Dismutase Mimetic Causes Rodent Tumor Regression and Vascular Destabilization. *Proceedings of the 94th Annual Meeting of the American Association for Cancer Research*, 2nd ed., 2003, **44**, 604.
21. (a) Hofseth, L. J.; Hussain, S. P.; Wogan, G. N.; Harris, C. C. Nitric oxide in cancer and chemoprevention. *Free Rad. Biol. Med.* **34**: 955-968; 2003. (b) Thomsen, L. L.; Miles, D. W. Role of nitric oxide in tumor progression: Lessons from human tumors. *Cancer Metastasis Rev.* **17**: 107-11; 1998.
22. Maulik, N.; Das, D. K. Redox signaling in vascular angiogenesis. *Free Radic. Biol. Med.* **33**: 1047-1060; 2002.
23. Vasquez-Vivar, J.; Martasek, P.; Whitsett, J.; Joseph, J.; Kalyanaraman, B. The ratio between tetrahydrobiopterin and oxidized tetrahydrobiopterin analogues controls superoxide release from endothelial nitric oxide synthase: an EPR trapping study. *Biochem. J.* **362**: 733-739; 2002.

24. Kinoshita, H.; Tsutsui, M.; Milstien, S.; Katusic, Z. S. Tetrahydrobiopterin, nitric oxide and regulation of cerebral arterial tone. *Prog. Neurobiol.* **52**: 295-302; 1997.
25. Okado-Matsumoto, A.; Batinic-Haberle, I.; Fridovich, I. The protection of SOD-deficient *E. coli* by *N*-alkylpyridylporphyrins. *Free Radic. Biol. Med.* In press.
26. Gorren, A. C. F.; Kungl, A. J.; Schmidt, K.; Werner, E. R.; Mayer, B. Electrochemistry of pterin cofactors and inhibitors of nitric oxide synthase. *Nitric Oxide: Biol. Chem.* **5**: 176-186; 2001.
27. Williams, N. H.; Yandell, J. K. Outer-sphere electron-transfer reactions of ascorbate anions. *Aust. J. Chem.* **35**: 1133-1144; 1982.
28. Koppenol, W. H. A thermodynamic appraisal of the radical sink hypothesis. *Free Radic. Biol. Med.* **14**: 91-94; 1993.
29. Trofimova, N. S.; Safronov, A. Y.; Ikeda, O. Electrochemical and spectral studies on the reductive nitrosylation of water-soluble iron porphyrin. *Inorg. Chem.* **42**: 1945-1951; 2003.
30. Kelly, S.; Lancon, D.; Kadish, K. M. Electron transfer and ligand addition reactions of (TPP)Mn(NO) and (TPP)Co(NO) in nonaqueous media. *Inorg. Chem.* **23**: 1451-1458; 1984.
31. Mu, X. H.; Kadish, K. M. In situ FTIR and uv-visible spectroelectrochemical studies of iron nitrosyl porphyrins in nonaqueous media. *Inorg. Chem.* **27**: 4720-4725; 1988.
32. Simic, M. G.; Jovanovic, S. V. Antioxidant mechanism of uric acid. *J. Am. Chem. Soc.* **111**: 5778-5782; 1989.
33. Archer, M. C.; Vonderschmitt, D. J.; Scrimgeour, K. G. Mechanism of oxidation of tetrahydrobiopterins. *Can. J. Biochem.* **50**: 1174-1182; 1972.
34. Ross, A. D.; Sheng, H.; Warner, D. S.; Piantadosi, C. A.; Batinic-Haberle, I.; Day, B. J.. Crapo, J. D. Hemodynamic Effects of Metalloporphyrin Catalytic Antioxidants: Structure-Activity Relationships and Species Specificity. *Free Radic. Biol. Med.* **33**: 1657-1669; 2002.
35. Vasquez-Vivar, J.; Hogg, N.; Martasek, P.; Karoui, H.; Pritchard, Jr. K. A.; Kalyanaramn, B. Tetrahydrobiopterin-dependent inhibition of superoxide generation from neuronal nitric oxide synthase. *J. Biol. Chem.* **274**: 26736-26742; 1999.
36. Vasquez-Vivar, J.; Whitsett, J.; Martasek, P.; Hogg, N.; Kalyanaram, B. Reaction of tetrahydrobiopterin with superoxide: EPR-kinetic analysis and characterization of the pteridine radical. *Free Radic. Biol. Med.* **31**: 975-985; 2001.
37. (a) Jones, C. L.; Vasquez-Vivar, J.; Griscavage, J.; Masters, B. S. S.; Martasek, P.; Kalyanaraman, B.; Gross, S. S. Only fully reduced pterins attenuate superoxide production by eNOS: an explanation for the tetrahydrobiopterin requirement? In Moncada. S.; Gustafsson, L.; Wiklund, P.; Higgs, E. A.; eds. *Biology of Nitric Oxide*, part 7. London: Portland Press; 2000, 118. (b) Raman, C. S., Martasek, P. Masters, B. S. S., Structural themes determining function in nitric oxide synthases, in Kadish, K. M., Smith, K. M., Guliard, R., eds., *The Porphyrin Handbook*, Vol. 4, Academic Press **2000**, 313-318.
38. Dulak. J.; Jozkowicz, A.; Dembinska-Kiec, A.; Guevara, I.; Zdzienicka, A.; Zmudzinska-Grochot, D.; Florek, I.; Wojtowicz, A.; Szuba, A.; Cooke, J. P. Nitric oxide induces the synthesis of vascular endothelial growth factor by rat vascular smooth muscle cells. *Arterioscler. Thromb. Vasc. Biol.* **20**: 659-666; 2000.
39. Ziche, M.; Morbidelli, L.; Choudhuri, R.; Zhang, H.-T.; Donnini, S.; Granger, H. J.; Bicknell, R. Nitric oxide synthase lies downstream from vascular endothelial growth factor-induced but not basic fibroblast growth factor-induced angiogenesis. *J. Clin. Invest.* **99**:2625-2634; 1997.
40. Shimizu, S.; Yasuda, M.; Ishii, M.; Nagai, T.; Kiuchi, Y.; Yamamoto, T. Stimulation of in vitro angiogenesis by tetrahydrobiopterin in bovine aortic endothelial cells. *Jpn. J. Pharmacol.* **80**: 177-180; 1999.
41. Sun, Y. Free radicals, antioxidant enzymes, and carcinogensis. *Free Radic. Biol. Med.* **8**: 583-599; 1990.
42. Dabrowska-Ufniarz, E.; Dzieniszewski, J.; Jarosz, M.; Wartanowicz, M.; Vitamin C concentration in gastric juice in patients with precancerous lesions of the stomach and gastric cancer. *Med. Sci. Monit.* **8**: CR96-103; 2002.
43. Kumaraguruparan, R.; Subapriya, R.; Kabalimoorthy, J.; Nagini, S. Antioxidant profile in the circulation of patients with fibroadenoma and adenocarcinoma of the breast. *Clin. Biochem.* **35**: 275-279; 2002.
44. Bozkir. A.; Simsek. B.; Gungor, A.; Torun, M. Ascorbic acid and uric acid levels in lung cancer patients. *J. Clin. Pharmacol. Therap.* **24**: 43-47; 1999.

45. Abiaka, C.; Al-Awadi, F.; Gulshan, S.; Al-Sayer, H.; Behbehani, A.; Farghaly, M.; Simbeye, A.; Plasma concentrations of alpha-tocopherol and urate in patients with different types of cancer. *J. Clin. Pharm. Therap.* **26**: 265-270; 2001.
46. (a) Jaruga, P.; Zastawny, T. H.; Skokowski J.; Dizdaroglu, M.; Olinski, R. Oxidative DNA base damage and antioxidant enzyme activities in human lung cancer. *FEBS Lett.* **341**: 59-64; 1994; (b) Kinnnula, V. L., Crapo, J. D. Superoxide dismutases in malignant cells and tumors. *Free Radic. Biol. Med.* 36: 718-744; 2004.
47. Patel, K. B.; Stratford, M. R. L.; Wardman, P.; Everett, S. A. Oxidation of tetrahydrobiopterin by biological radicals and scavenging of the tetrahydrobiopterin radical by ascorbate. *Free Radic. Biol. Med.* **32**: 203-211; 2002.
48. Kokolis, N., Ziegler, I., On the levels of phenylalanine, tyrosine and tetrahydrobiopterin in the blood of tumor-bearing organism. *Cancer Biochem. Biophys.* **2**: 79-85; 1977.
49. Shang, T.; Kotamraju, S.; Kalivendi, S. V.; Hillard, C. J.; Kalyanaramn, B. 1-Methyl-4-phenylpyridinium-induced apoptosis in cerebellar granule neurons is mediated by transferrin receptor iron-dependent depletion of tetrahydrobiopterin and neuronal nitric oxide synthase-derived superoxide. *J. Biol. Chem* .published on-line, January, 2004.

Schemes

Scheme I. Mn(III) porphyrins studied.
Scheme II. Tetrahydrobiopterin (BH_4) and its oxidized analogues.

Figures

Figure 1. The uv/vis spectroscopy of the interaction of Mn porphyrins with tetrahydrobiopterin (BH_4) (**A**) and its oxidized derivatives, 7,8-dihydrobiopterin (7,8-BH_2) (**B**) and L-sepiapterin (sep) (**B-inset**): (**A**) The spectra of 5 μM Mn^{III}TE-2-PyP^{5+} (E) and 3 μM Mn^{III}TnOct-2-PyP^{5+} (nOct) were taken in the presence and absence of 0.3 mM BH_4 in PBS, pH 7.4, at 25 ± 1°C. (**B**) The 5 μM Mn^{III}TE-2-PyP^{5+} was reduced by 12 μM ascorbic acid followed by the addition of 0.4 mM 7,8-BH_2 in PBS, pH 7.4, at 25 ± 1°C. (**B-inset**) The 5 μM Mn^{III}TE-2-PyP^{5+} was reduced by 12 μM ascorbic acid followed by the addition of 0.3 mM L-sepiapterin in PBS, pH 7.4, at 25 ± 1°C. The interaction was performed under anaerobic conditions obtained by purging argon for 15 min.

Figure 2. Catalytic oxidation of BH_4 with 5 μM Mn^{III}TE-2-PyP^{5+} (E) and MnTnOct-2-PyP^{5+} (nOct) in PBS, pH 7.4, at 25 ± 1°C. Catalytic action was enabled through reoxidation of Mn(II) porphyrin by oxygen. In one experiment, first the 0.35 mM BH_4 was added into phosphate buffer followed by the addition of MnTE-2-PyP^{5+} (E, **dotted line**) or MnTnOct-2-PyP^{5+} (nOct, **solid line**) as indicated. After ~200 s, and with MnTE-2-PyP^{5+}, another 0.73 mM BH_4 was added to assure that enough reductant was present. Finally, ~2 mg of $Na_2S_2O_4$ was added to assure removal of all oxygen. **Dash line:** In another experiment, first 5 μM MnTE-2-PyP^{5+} (E) was added into phosphate buffer, followed by the addition of 0.9 mM BH_4 as indicated. Finally, ~ 2mg of $Na_2S_2O_4$ was added as noted.

Figure 3. Plots of the observed pseudo-first order rate constant, k_{obs} *vs* BH_4 concentration for the reduction of MnTE-2-PyP^{5+} with BH_4. Stopped-flow kinetics were done anaerobically with 6 μM MnTE-2-PyP^{5+} and 30 - 600 μM BH_4 in PBS buffer, pH 7.4, and at 25 ± 0.1 °C.

Scheme I

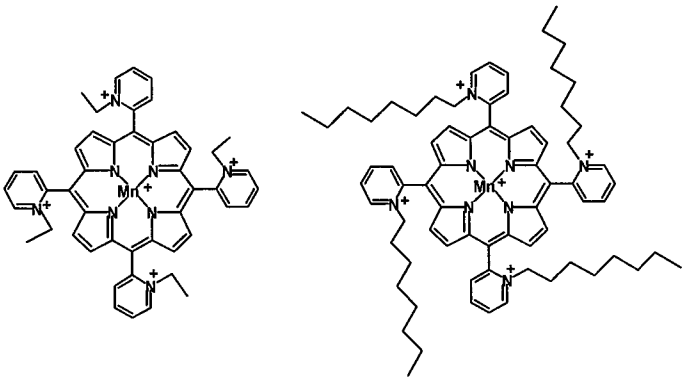

Mn^{III}TE-2-PyP^{5+} Mn^{III}TnOct-2-PyP^{5+}

Scheme II

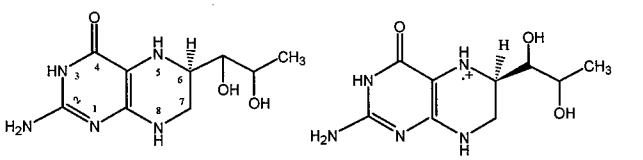

(6R)-Tetrahydrobiopterin, BH_4 (6R)-Tetrahydrobiopterin radical, $BH_4^{\cdot+}$

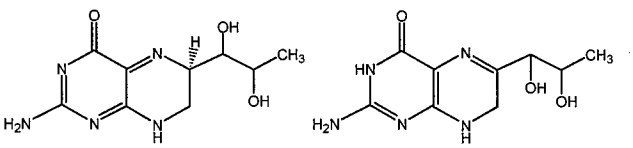

6,7-dihydro-8*H*-biopterin, 6,7-BH_2 7,8-dihydrobiopterin, 7,8-BH_2

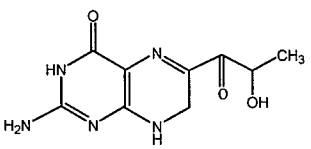

Sepiapterin

Figure 1

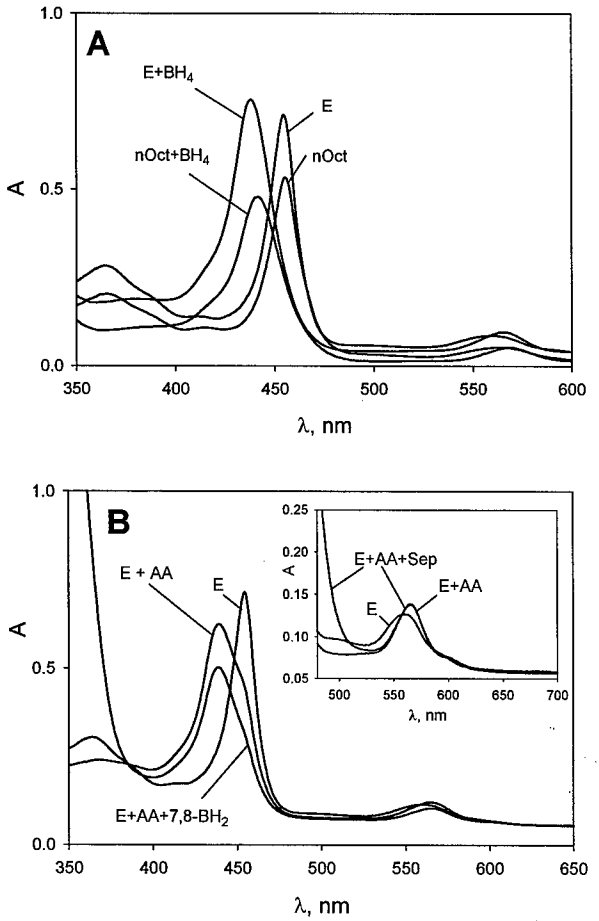
A
E+BH4
E
nOct+BH4
nOct
A
1.0
0.5
0.0
350
400
450
500
550
600
λ, nm
B
E + AA
E
E+AA+7,8-BH2
E+AA+Sep
E+AA
E
A
0.25
0.20
0.15
0.10
0.05
500
550
600
650
700
λ, nm
1.0
0.5
0.0
350
400
450
500
550
600
650
λ, nm

Figure 2

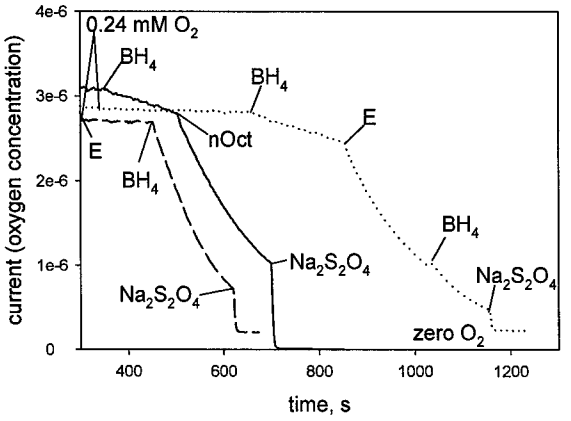

Figure 3

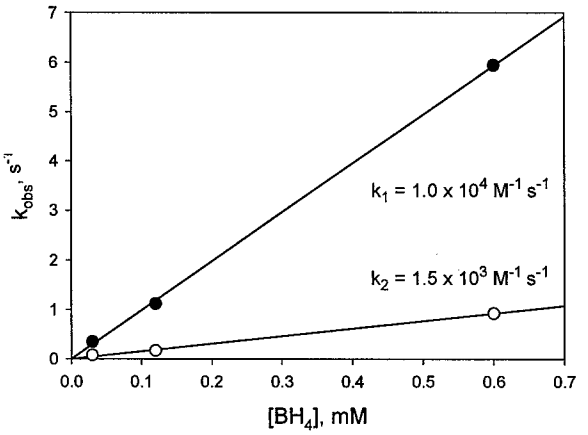

2. *Int. J. Rad. Oncol. Biol. Phys.* Submitted, **2004**

Effects of a Catalytic Metalloporphyrin Antioxidant on Tumor Radioresponsiveness

by
Benjamin J. Moeller,[1] Ines Batinic-Haberle,[1] Ivan Spasojevic,[2] Zahid N. Rabbani,[1] Mitchell S. Anscher,[1] Zeljko Vujaskovic,[1] and Mark W. Dewhirst[1,3]

[1]Department of Radiation Oncology, Duke University Medical Center, Durham, NC, USA
[2]Department of Medicine, Duke University Medical Center, Durham, NC, USA
[3] Communicating Author
Room 201 MSRB
Research Drive
PO Box 3455
Duke University Medical Center
Durham, NC 27710
dewhirst@radonc.duke.edu
p: (919) 684-4180
f: (919) 684-8718

Running Title: Manganese Porphyrin Antioxidant and Tumor Radiosensitivity
Key Words: manganese porphyrin, antioxidant, superoxide dismutase, radiotherapy
Acknowledgements: Work supported by Incara Pharmaceuticals, by NIH grants CA40355 (MWD), P30CA14236 (ZV), and by DOD CDMRP grant BC024326 (IBH).

Abstract

Purpose: Studies have shown that a catalytic antioxidant, Mn(III) tetrakis(*N*-ethylpyridinium-2-yl)porphyrin ($MnTE\text{-}2\text{-}PyP^{5+}$), can suppress both late normal tissue radiation injury and tumor growth. What effect it might have on tumor radioresponsiveness has yet to be determined.
Methods: Various rodent tumor and endothelial cells lines were exposed to $MnTE\text{-}2\text{-}PyP^{5+}$ and assayed for viability and radiosensitivity *in vitro*. Next, tumors were treated with radiation and $MnTE\text{-}2\text{-}PyP^{5+}$ *in vivo*, and the effects on tumor growth and vascularity were monitored.
Results: *In vitro*, $MnTE\text{-}2\text{-}PyP^{5+}$ had minimal impact on the viability and radiosensitivity of various tumor and endothelial cell lines. However, it significantly inhibited the ability of tumor cells to secrete factors capable of rescuing irradiated endothelial cells. *In vivo*, combined treatment with radiation and $MnTE\text{-}2\text{-}PyP^{5+}$ resulted in synergistic anti-tumor effects, irrespective of treatment sequencing or the duration of drug dosing. Co-treatment of tumors also achieved synergistic tumor devascularization, resulting in near complete destruction of the pre-existing tumor vasculature.
Conclusion: These studies support the conclusion that $MnTE\text{-}2\text{-}PyP^{5+}$ can protect normal tissues from radiation injury while improving tumor control, through augmenting radiation-induced damage to the tumor vasculature.

Introduction

Normal tissue toxicity remains a major limiting factor for escalating radiation doses to better treat tumors. Chemical radioprotection offers the promise of minimizing dose-limiting normal tissue radiotoxicity without compromising tumor control. Classic radioprotectors are designed to interfere with the damaging free radical cascades initiated by radiation (1). They are often selectively beneficial for normal tissues due to differences in either uptake or target sensitivity between normal and malignant cells (2, 3). Many antioxidants, both naturally-occurring and synthetic, have demonstrated significant capacity to protect normal tissues from radiation injury (4, 5).

As more has been learned about how oxidative stress promotes normal tissue radiotoxicity, new opportunities for radioprotection have arisen. It has long been recognized that free radicals initiate radiation-induced cellular damage (6). More recent studies have suggested that oxidative stress continues to promote radiation-induced damage long after normal tissues are irradiated (7, 8). As these later free radical-mediated signals are involved in natural physiologic/pathophysiologic processes, they might respond well to natural cellular antioxidants.

The superoxide dismutase (SOD) enzymes have received attention as potential natural radioprotectors. The three known forms of SOD all serve to catalyze the dismutation of superoxide to H_2O_2 and O_2 (9). They are localized within and outside the cell, are widely expressed throughout the body, and are important in redox homeostasis (10-12). Preclinical models have demonstrated that treating irradiated rodents with exogenous SOD – delivered by injection of the enzyme or through liposome or viral-

mediated gene therapy – can ameliorate radiation-induced pneumonitis (13-18). The same principle has also been demonstrated in transgenic mice overexpressing SOD in type II pneumocytes (19). Although these studies generated promising results, the difficulties of delivering SOD to target tissues, using gene therapy or otherwise, have somewhat impeded translation into the clinic.

To exploit the benefits of SOD administration while bypassing delivery and antigenicity problems, small molecular weight mimetics of the enzyme have been synthesized (20, 21). The structure-activity relationship was established between their superoxide dismuting ability and metal-centered redox potential (20, 21). The most potent compounds are positively charged *ortho* isomers of Mn(III) tetrakis(*N*-alkylpyridinium-2-yl)porphyrin, alkyl being methyl to n-octyl (22), Mn(III) tetrakis(*N*-alkylimidazolium-2-yl)porphyrin and their methoxyethyl derivatives (21). Besides catalytically eliminating superoxide, these compounds effectively scavenge other reactive oxygen and nitrogen species (ROS/RNS) while utilizing cellular reductants to assure the catalytic mode of their actions. The ethyl porphyrin, MnTE-2-PyP^{5+} dismutes superoxide with log k_{cat} = 7.76 (20, 22), reduces peroxynitrite with log k_{red} = 7.53 (23), reduces carbonate radical with log k_{red} = 8.49 (23), and oxidizes nitric oxide with log k_{ox} = 6 (24). MnTE-2-PyP^{5+} has been shown to prevent pathology in a wide variety of preclinical models of diseases wherein oxidative stress plays a role, including stroke (25-27), diabetes (28), and sickle cell anemia (29). In addition to directly eliminating ROS/RNS, MnTE-2-PyP^{5+} was recently shown to have various signaling effects which could modulate oxidative stress injuries in diseases such as cancer and diabetes (30, 31). This compound blocks DNA binding by the transcription factors NF-κB and AP-1, inhibiting downstream expression of important factors such as tumor necrosis factor and interleukin-1β (31, 32). Relevant to the current study, systemic administration of MnTE-2-PyP^{5+} has also been shown to protect against pathological and functional radiation pneumonitis, supporting the concept that SOD-based therapeutics might serve as clinically useful radioprotectors (33).

As is the case for all radioprotectors, it is important to consider what effects MnTE-2-PyP^{5+} might have on tumor radiosensitivity. There is convincing evidence in the literature to support the hypothesis that ROS/RNS are capable of promoting vascular angiogenesis (34), and that antioxidants have antiangiogenic activity (35-40). Also, a growing body of evidence suggests that antiangiogenic compounds act synergistically with radiotherapy by increasing radiation damage to the vasculature, leading to secondary tumor cell kill (41). Recently, it has been shown that MnTE-2-PyP^{5+} is capable of catalytically depleting tetrahydrobiopterin, a cofactor of nitric oxide synthase, thereby inhibiting an important source of angiogenesis-stimulating RNS. The ability to lower levels of nitric oxide, by direct depletion of tetrahydrobiopterin levels or through downregulation of NF-κB-mediated inducible NOS expression, may lend the compound anti-angiogenic activity (42). Taken together, these studies raise the possibility that MnTE-2-PyP^{5+} may improve radiotherapeutic control of tumors through an antivascular mechanism.

Based on the aforementioned data, we hypothesized that the normal tissue radioprotector, MnTE-2-PyP^{5+}, might enhance tumor radiosensitivity by augmenting destruction of the tumor vasculature. We used a combination of *in vitro* and *in vivo* assays to test the feasibility of combining MnTE-2-PyP^{5+} with radiotherapy. These

studies may validate the potential utility of MnTE-2-PyP^{5+} in the setting of tumor radiotherapy.

Materials and Methods

Cell Lines and Cell Culture 4T1 (mouse mammary carcinoma), B16 (mouse melanoma), R3230 (rat mammary carcinoma), and SVEC (SV40 large T antigen-transformed murine endothelial cell) lines were acquired from ATCC and grown in Dulbecco's Modified Eagle Medium (Gibco-BRL) with 10% Fetal Bovine Serum (Gibco-BRL) and penicillin-streptomycin (Gibco-BRL) at 5%CO_2 and 21%O_2.

Drug Synthesis MnTE-2-PyP^{5+} was prepared as previously described (43).

Clonogenic Assay Cells were harvested and incubated in a single-cell suspension with the desired concentration of MnTE-2-PyP^{5+} for 2 hours at 37°C. Cells were then placed in a Mark IV Cesium Irradiator (dose rate = 7 Gy/min, JL Shepherd, San Fernando, CA) on a rotating platform, and irradiated with predetermined doses. Immediately following irradiation, serial dilutions of the treated cells were plated in 6-well plates, each in triplicate. After incubating 9 days, colonies ($\geq$50 cells) were fixed, stained with crystal violet, and counted.

Viability Assay Cells were plated into 96-well dishes at a density of 10^3 cells per well in typical growth media. 12 hours later, MnTE-2-PyP^{5+} was added at the desired concentration. After predetermined incubation periods methylthiazolyldiphenyl-tetrazolium (MTT, Sigma) was added to each well to a final concentration of 1mg/mL. 4 hours later, the media was removed, MTT crystals were dissolved in 100% dimethylsulfoxide, and the optical density was read on a spectrophotometer (OD_{570}).

Endothelial Radioprotection Assay Sub-confluent 4T1 cells were incubated at 0.5% O_2 for 12 hours with or without MnTE-2-PyP^{5+} to generate conditioned media. Conditioned media was then collected, and MnTE-2-PyP^{5+} was added to the previously drug-free samples. Endothelial cells were plated as for viability assays. 12 hours later, the media was replaced with MnTE-2-PyP^{5+}-containing conditioned media. 2 hours later, the cells were irradiated as described above. 96 hours following treatment, cells underwent a viability assay, as described above. Endothelial cell viability was determined from MTT results according to methodology described previously (44). Briefly, spectrophotometric results were normalized according to the following equation:

$$V_{RxMy} = (A_{RxMy} - A_0)/(A_{My} - A_0)$$

where V_{RxMy} is the relative viability of the cells treated with predetermined doses of radiation (Rx) and MnTE-2-PyP^{5+} (My), A_{RxMy} is the MTT absorbance of those cells, A_{My} is the MTT absorbance of the unirradiated controls treated with the same dose of MnTE-2-PyP^{5+}, and A_0 is the MTT absorbance of the cells prior to treatment.

Animals Female Fisher-344 rats, C57/Bl6 mice, and Balb/C mice were housed and treated in accordance with approved guidelines from the Duke University Institutional Animal Care and Use Committee.

Tumors 4T1 tumors were grown in the flank of Balb/C mice by injecting a single cell suspension of tumor cells (10^5). Tumor volumes were measured with calipers and calculated based on two diameters according to the formula: $v = (a^2*b)/2$, where v is the volume, a is the short diameter, and b is the long diameter. Animals were sacrificed once tumors reached five times their initial treatment volumes.

Skinfold Window Chambers Window chambers were implanted as described previously (45). Briefly, mice were anesthetized with nembutal (80 mg/kg, intraperitoneal), and a 1cm diameter circular incision was made in the dorsal skin flap over which a titanium chamber was surgically implanted. A 10μl suspension of tumor cells ($5x10^3$ cells) was then injected into the opposing flap of skin. A circular cover slip was placed over the incision through which the vasculature, tissue, and tumor cells were visualized. Observations of window chamber tumors were performed daily on restrained, unanesthetized mice using an inverted Zeiss fluorescence microscope. Images were captured onto a PC using Scion Image software (Frederick, MD), and analyzed using Adobe Photoshop (San Jose, CA). Tumor volume and vascular length densities were calculated as described previously (46). Briefly, tumor volumes were calculated using the formula: $d^2(3.14/2)$, where the diameter was determined from low-power (2.5X) microscopy images by comparing pixel dimensions to micrometer values. Vascular length densities were measured from medium-power (5X) fields by using image analysis software (Scion Image) to trace the vascular network. Measurement of the sum length of all vessels within each tumor was then determined, in pixels, and converted to metric length by comparing pixel dimensions to micrometer values.

Tumor Irradiation Animals were randomized to treatment groups once flank tumors reached a mean volume of $200mm^3$ (n = 5/group), and window chamber tumors were 1mm in diameter (n = 5/group). Tumor-bearing Balb/C mice were restrained, unanesthetized, in a plastic tube and placed in a Mark IV Cesium irradiator (dose rate = 7 Gy/min, JL Shepherd, San Fernando, CA). The mice were positioned behind a lead shield allowing only the tumor-bearing area to remain in the treatment field. Three doses of 5 Gy were administered, separated by 12 hours each.

Statistics Unless otherwise noted, data are reported as a mean +/- standard deviations. Statistical significance was determined using a Students' t test or ANOVA, where appropriate, and *P* values less than 0.05 were considered significant.

Results

MnTE-2-PyP^{5+} Lacks Cytotoxicity *In Vitro* To determine whether MnTE-2-PyP^{5+} might be toxic to tumor and/or endothelial cells (ECs), 4T1, B16, R3230, and SVEC cells were grown in the presence of the drug at concentrations typically required for efficacy in treated cells (47), and cellular viability was measured at regular time intervals using an MTT assay. MnTE-2-PyP^{5+}, at concentrations of 1, 2, and 5 μM, had significant growth inhibitory effects on 4T1 and R3230 tumor cells during the first 24 hours of exposure (Figure 1A). As incubation times increased, however, the cytotoxicity of the compound was less apparent. After a period of 48 hours there were no significant effects of MnTE-2-PyP^{5+} on proliferation/viability for any of the cell lines examined (Figure 1B). Similar negative results were seen for incubation times of 72 and 96 hours (data not shown).

Tumor Radiosensitivity is Unaffected by MnTE-2-PyP^{5+} *In Vitro* The two tumor cell lines displaying more apparent sensitivity to MnTE-2-PyP^{5+}, 4T1 and R3230 (Figure 1A), were next used in a clonogenic assay to determine whether the compound acts as a cellular radioprotectant. MnTE-2-PyP^{5+} (5μM) was administered two hours before irradiation, and removed 30 minutes afterwards to minimize the effects of the

drug, itself, on cellular viability. The survival curves for both cell lines were largely identical with or without MnTE-2-PyP^{5+}, suggesting that the compound does not directly protect tumor cells from ionizing radiation (Figure 2A). Similarly, the viability of endothelial cells was not affected by irradiating in the presence of MnTE-2-PyP^{5+} (Figure 2B), using the same experimental design as with the tumor cells, above.

MnTE-2-PyP^{5+} Inhibits EC Radioprotection As vascular radiosensitivity may significantly impact overall tumor radioresponsiveness (48), we next examined the possibility that MnTE-2-PyP^{5+} might influence radiotherapy through modulating EC radiosensitivity. Since tumor cells secrete cytokines which can diminish EC responsiveness to radiation damage (49), EC radiosensitivity might be affected by MnTE-2-PyP^{5+} acting on tumor *or* endothelial cells. Thus, conditioned media was made one of two ways: 1) by culturing tumor cells in hypoxic conditions with MnTE-2-PyP^{5+}, or 2) by culturing tumor cells in hypoxic conditions without drug, followed by the addition of MnTE-2-PyP^{5+} to the conditioned media after it was collected. This way, the influence of the compound on tumor cells and endothelial cells could be differentiated. These samples were then added to adherent ECs two hours prior to irradiation. EC viability was determined 96 hours post-irradiation, corresponding to the time of maximum vascular destabilization after tumor irradiation *in vivo* (49).

Consistent with our previous findings (49), tumor-conditioned media caused irradiated ECs to be significantly more viable (Figure 3). Adding MnTE-2-PyP^{5+} to the media after it had been conditioned had no impact on the media's ability to rescue irradiated ECs. However, media that was conditioned in the presence of MnTE-2-PyP^{5+} was significantly less capable of rescuing ECs in this way. The addition of as little as 2μM MnTE-2-PyP^{5+} blocked the ability of tumor cells to secrete EC-rescuing factors into the media, causing the endothelial cells to behave identically to those incubated with non-conditioned growth media.

MnTE-2-PyP^{5+} Enhances Radiation-Induced Tumor Growth Delay To determine how combined treatment with radiation/MnTE-2-PyP^{5+} would impact tumor growth, 4T1 tumors were grown in the flank, randomized to treatment with radiation or sham-irradiation, and PBS or MnTE-2-PyP^{5+}, and followed by caliper measurements (n = 5/group). Two sequencing schemes were used for delivering the combined treatments: *1)* MnTE-2-PyP^{5+} (6mg/kg) administered one hour prior to each of three radiation doses, or *2)* MnTE-2-PyP^{5+} (6mg/kg) administered 1, 13, and 25 hours after the final radiation dose. Note that for the combined treatment groups, dose and dosing intervals were identical, and only sequencing was changed. If MnTE-2-PyP^{5+} were to act as a direct radioprotectant (e.g. ROS/RNS scavenger) for the tumor or its vasculature, it would be expected that the drug-first sequence would affect tumor growth delay differently than the radiation-first sequence. What was found, however, was that tumor growth delay was identical in the combined modality groups, irrespective of sequencing (Figure 4). Moreover, radiation plus MnTE-2-PyP^{5+} resulted in significant improvement in tumor response compared to that seen with each treatment modality, alone ($P < 0.01$). These data suggest that MnTE-2-PyP^{5+} does not act as a direct radioprotectant for tumor tissue and, indeed, may in fact enhance tumor radioresponsiveness.

MnTE-2-PyP^{5+} Enhances Radiation Injury to Tumor Vessels To understand the mechanism behind the enhancement of radiation efficacy with MnTE-2-PyP^{5+}, we

next investigated whether MnTE-2-PyP^{5+} would radiosensitize tumor-associated vasculature *in vivo*, as predicted by our *in vitro* studies. 4T1 tumors were grown in dorsal skinfold window chambers, allowing serial observation of tumor vascularity. Once tumors reached a predetermined size (1mm diameter), they were randomized to treatment with PBS or MnTE-2-PyP^{5+}, and radiation or sham-irradiation (n = 5/group). Immediately after (sham-) irradiation, daily injections of PBS or MnTE-2-PyP^{5+} began and continued for 48 hours (three doses total, 6mg/kg). Intravital microscopy was used daily to measure the vascular length density of the window chamber tumors, carried at 0, 24, 48, and 72 hours following (sham-) irradiation (Figure 5). Neither PBS nor MnTE-2-PyP^{5+} alone had an effect on tumor vascularity over the course of the experiment. There was a non-significant trend towards increased vessel density in the radiation alone group. In the combined treatment group, however, there was a striking tumor devascularization beginning at 48 hours post-radiation and peaking 24 hours later. After MnTE-2-PyP^{5+} injections were discontinued, tumor vascularity gradually recovered (data not shown).

Discussion

This study demonstrates that MnTE-2-PyP^{5+}, previously shown to protect lung tissue from radiation injury (33), might be a useful adjunct to radiotherapy without the risk of diminishing tumor radioresponsiveness. Our findings suggest that SOD mimetics may significantly augment the therapeutic index of radiotherapy by not only protecting normal tissues, but also by enhancing radiation-induced damage to some tumors. Also, the apparent role for MnTE-2-PyP^{5+} in targeting irradiated tumor vasculature adds to our understanding of the relationship between radiation and angiogenesis, and how their interplay might be exploited for therapeutic benefit.

Several conclusions can be drawn out of the data presented here. First, these studies suggest that the biologically-relevant effects of MnTE-2-PyP^{5+} in irradiated tissues are likely due to activity occurring after radiation has been delivered. Contrary to what might have been expected, in none of our studies was it found that pre-radiation treatment with MnTE-2-PyP^{5+} impacted outcome any differently than post-radiation treatment did. As antioxidants have long been presumed to interfere with the initial free radical burst coincident with irradiation (4), the post-radiation effects of MnTE-2-PyP^{5+} seem somewhat paradoxical. However, these findings are consistent with recent evidence showing that reactive oxygen and/or nitrogen species may be important in the delayed response to radiation damage in both normal and tumor tissue.

Several studies have demonstrated that normal tissues experience significantly elevated levels of intracellular ROS/RNS between one to two weeks following irradiation (50, 51). Also, our previous studies have provided direct proof that tumor ROS/RNS are significantly increased 1-2 days after radiation, providing further support for the hypothesis that oxidative stress may play a role in the delayed effects of ionizing radiation (49). This long-lived oxidative stress may be involved in promoting genotoxicity and differential signaling pathway regulation in irradiated tissues. This paradigm would provide a role for antioxidants, such as MnTE-2-PyP^{5+}, in influencing radiation outcome in the post-irradiation period. Our studies provide strong evidence that catalytic antioxidants can improve tumor radiosensitivity by decreasing ROS/RNS levels in the post-radiation period. This highlights the importance of delayed oxidative stress in

the tumor response to radiation, and identifies ROS/RNS as potential targets in an unknown number of important radiation-induced tumor signaling cascades. Further refining this hypothesis, we have shown that the major impact of post-radiation antioxidant activity is a significant reduction in vascular viability within the irradiated tumor. Given the high level of current interest in antiangiogenic therapeutics, and in combining antiangiogenic approaches with radiotherapy, these are intriguing findings.

Although very little is known about the role oxidative stress plays in promoting vascular radioresistance, much more is known about the interplay between ROS/RNS and angiogenesis. Since many of the same signaling pathways are used in both processes, these data may help to explain the results seen here. Levels of oxidative stress are typically high in tumors (52-55). Highly oxidative environments tend to promote angiogenesis by stimulating angiogenic cytokine secretion (56-58), lymphocyte-induced vascular morphogenesis (59), and by directly promoting endothelial tubular morphogenesis (57, 60), providing mechanistic links between oxidative stress and tumor angiogenesis. Our data indicates that MnTE-2-PyP^{5+} may interfere with this relationship by disrupting ROS/RNS-induced cytokine secretion from tumor cells (Figure 3). Which cytokines are being inhibited by MnTE-2-PyP^{5+} here is not yet known – however, the existing literature on the subject provides some clues. Both ROS and RNS have been implicated in upregulating hypoxia-inducible factor-1 (61-64), which stimulates the production of a variety of pro-angiogenic cytokines, including vascular endothelial growth factor (VEGF) (65). Oxidants may also be involved in stimulating NF-κB and AP-1 signaling (66, 67), both of which can stimulate vascular signaling in hypoxic tumors (34). For irradiated tumors, in particular, ROS/RNS stimulate activation of hypoxia-inducible factor-1 (HIF-1), serving to stimulate expression of a variety of endothelial cell-active cytokines which, in turn, promote endothelial radioresistance (49). As MnTE-2-PyP^{5+} has been shown to be able to block AP-1, NF-κB, and HIF-1 signaling (31, 32, 49), it seems clear that the compound is well-equipped to inhibit ROS/RNS-induced cytokine (VEGF, etc.) release from tumor cells. These data form a clear framework to explain how oxidative stress in tumors promotes vascular resistance to ionizing radiation. The studies presented here are consistent with this model wherein tumor cells are the site of ROS/RNS of vascular signaling. MnTE-2-PyP^{5+} is clearly able to inhibit the capacity for tumor cells to induce radioprotection in endothelial cells, allowing it to impact vascular radioresistance at a distance.

Further, these studies demonstrate that MnTE-2-PyP^{5+} is equally efficacious when administered before/during radiotherapy as compared to its efficacy when given afterwards. From this, it can be concluded that the anti-tumor radiosensitizing effects of MnTE-2-PyP^{5+} outweigh any potential radioprotection which might occur during combined treatment *in vivo*. Supporting this conclusion, our *in vitro* experiments show no evidence that MnTE-2-PyP^{5+} alters the intrinsic radiosensitivity of tumor cells at clinically relevant doses. Since MnTE-2-PyP^{5+} clearly serves as a ROS/RNS scavenger in tumor cells at such doses (49), these results were surprising. There are several putative explanations for why MnTE-2-PyP^{5+} might not serve as a scavenger for oxidative stress in this situation (irradiation), when it clearly does so in others (diabetes, stroke, etc.), including differences in the concentration and species of the drug's target, as well as the drug's localization. The existing data support the conclusion that MnTE-2-PyP^{5+} is equipped to handle a high level and broad diversity of ROS/RNS (see Introduction), such

that the oxidative species initiated by ionizing radiation ought to be within the capacity of the compound to scavenge. What is less certain is whether any significant portion of the MnTE-2-PyP^{5+} taken up by a cell is localized within the nucleus. For the drug to impact the clonogenicity of the irradiated cell, efficient delivery to the nucleus – and proximity to the DNA therein – would be required. Although formal studies of subcellular compartmentalization are yet to come, *in vitro* evidence suggests that association between MnTE-2-PyP^{5+} and nucleic acids is poor, and that access to membrane-bound cellular organelles may be limited (personal communication, Ines Batinic-Haberle). Further studies into the impact of MnTE-2-PyP^{5+}'s cellular compartmentalization are warranted to clarify this issue.

Since this compound has been shown to be an effective normal tissue radioprotectant, preclinically (33), our studies here provide further justification for exploring its utility in clinical radiation oncology. With the potential to simultaneously protect normal tissues while radiosensitizing tumors, MnTE-2-PyP^{5+} may prove to be a valuable adjunct to radiotherapy.

Figure Legends

Figure 1. MnTE-2-PyP^{5+} Lacks Overt Cytotoxicity Four cell lines were exposed to various concentrations of MnTE-2-PyP^{5+} for **(A)** 24 or **(B)** 48 hours, and assayed for viability using an MTT assay. For each cell line, results were normalized to measured values for control cells not exposed to MnTE-2-PyP^{5+}. The compound exhibited transient effects on cellular viability for 4T1 and R3230 cells. Viability following 72 and 96 hours of drug exposure was similar to that for 48 hours (not shown). Error bars represent standard deviation. * = $P < 0.05$ versus drug-free control.

Figure 2. MnTE-2-PyP^{5+} Fails to Radioprotect *In Vitro* 4T1, R3230 **(A)**, and SVEC cells **(B)** were irradiated in the presence of 0 or 5μM concentrations of MnTE-2-PyP^{5+}. Clonogenicity was identical for each line regardless of whether or not drug was present. Results are normalized by plating efficiency of non-irradiated controls, and plotted as the average of three samples for each data point. Error bars represent standard deviation.

Figure 3. MnTE-2-PyP^{5+} Inhibits EC Radioprotection by Tumor Cells 4T1 cells were incubated at 0.5% O_2 for 24 hours, and the overlying media was collected for further studies. Conditioned media was either generated in the presence of MnTE-2-PyP^{5+} (Pre-Incubation), or was supplemented with the drug after media collection (Post-Incubation). Endothelial cells were cultured in Pre-Incubation conditioned media, Post-Incubation conditioned media, or unconditioned growth media from 2 hours prior to irradiation (10 Gy), until 96 hours later when EC viability was determined by MTT assay. Results were normalized to growth media-incubated, non-irradiated controls. Error bars represent standard deviation. * = $P < 0.05$ versus growth media-incubated, irradiated control.

Figure 4. MnTE-2-PyP^{5+} Enhances Tumor Radiosensitivity *In Vivo* 4T1 tumors were grown in the flank, allowed to reach ≥ 200mm^3 in size, and 25 tumors were randomized evenly to one of five treatment groups on day 9 post-implantation: *1)* PBS, *2)* MnTE-2-PyP^{5+} (6mg/kg every 12 hours X3), *3)* RT (5Gy every 12 hours X3), *4)* "MnTE-2-PyP+RT" (one MnTE-2-PyP^{5+} dose prior to each fraction of radiation), or *5)* "RT+ MnTE-2-PyP" (three MnTE-2-PyP^{5+} doses following third fraction of radiation). The

combined treatment groups had significant, supra-additive effects on radiation-induced tumor growth delay, irrespective of sequencing. n = 5/group. * = $P < 0.01$. Error bars represent standard deviation.

Figure 5. MnTE-2-PyP^{5+} Enhances Radiosensitivity of Tumor Vasculature *In Vivo* 4T1 window chamber tumors were randomized to treatment with PBS or MnTE-2-PyP^{5+}, and radiation or sham-irradiation. A course of three fractions of radiation (5 Gy each, 12 hours apart) was followed immediately by daily administration of MnTE-2-PyP^{5+} (6mg/kg/day) for three days. Tumors were imaged immediately after radiation (0 hours), and every day thereafter (24, 48, and 72 hours), and these images were used to calculate the tumor vascular length densities. Combined treatment resulted in significant tumor devascularization between 48 and 72 hours post-radiation. n = 5/group. * = $P < 0.05$ vs. "0 hour" tumor VLD.

References

1. Stewart FA. Modification of normal tissue response to radiotherapy and chemotherapy. *Int J Radiat Oncol Biol Phys* 1989;16:1195-1200.
2. Zhang X, Lai PP, Taylor YC. Differential radioprotection of cultured human diploid fibroblasts and fibrosarcoma cells by WR1065. *Int J Radiat Oncol Biol Phys* 1992;24:713-719.
3. Quinones HI, List AF, Gerner EW. Selective exclusion by the polyamine transporter as a mechanism for differential radioprotection of amifostine derivatives. *Clin Cancer Res* 2002;8:1295-1300.
4. Weiss JF, Landauer MR. Radioprotection by antioxidants. *Ann N Y Acad Sci* 2000;899:44-60.
5. Weiss JF, Landauer MR. Protection against ionizing radiation by antioxidant nutrients and phytochemicals. *Toxicology* 2003;189:1-20.
6. Riley PA. Free radicals in biology: oxidative stress and the effects of ionizing radiation. *Int J Radiat Biol* 1994;65:27-33.
7. Jack CI, Cottier B, Jackson MJ, *et al.* Indicators of free radical activity in patients developing radiation pneumonitis. *Int J Radiat Oncol Biol Phys* 1996;34:149-154.
8. Bai YH, Wang DW, Wang LP, *et al.* The role of free radicals in the development of radiation interstitial pneumonitis. *J Environ Pathol Toxicol Oncol* 1993;12:199-204.
9. Fridovich I. Superoxide dismutases. *Annu Rev Biochem* 1975;44:147-159.
10. Fattman CL, Schaefer LM, Oury TD. Extracellular superoxide dismutase in biology and medicine. *Free Radic Biol Med* 2003;35:236-256.
11. Kinnula VL, Crapo JD. Superoxide dismutases in the lung and human lung diseases. *Am J Respir Crit Care Med* 2003;167:1600-1619.
12. Noor R, Mittal S, Iqbal J. Superoxide dismutase--applications and relevance to human diseases. *Med Sci Monit* 2002;8:RA210-215.
13. Malaker K, Das RM. Effect of superoxide dismutase on early radiation injury of lungs in the rat. *Mol Cell Biochem* 1988;84:141-145.
14. Breuer R, Tochner Z, Conner MW, *et al.* Superoxide dismutase inhibits radiation-induced lung injury in hamsters. *Lung* 1992;170:19-29.

15. Epperly MW, Bray JA, Krager S, *et al.* Intratracheal injection of adenovirus containing the human MnSOD transgene protects athymic nude mice from irradiation-induced organizing alveolitis. *Int J Radiat Oncol Biol Phys* 1999;43:169-181.
16. Stickle RL, Epperly MW, Klein E, *et al.* Prevention of irradiation-induced esophagitis by plasmid/liposome delivery of the human manganese superoxide dismutase transgene. *Radiat Oncol Investig* 1999;7:204-217.
17. Epperly M, Bray J, Kraeger S, *et al.* Prevention of late effects of irradiation lung damage by manganese superoxide dismutase gene therapy. *Gene Ther* 1998;5:196-208.
18. Epperly MW, Epstein CJ, Travis EL, *et al.* Decreased pulmonary radiation resistance of manganese superoxide dismutase (MnSOD)-deficient mice is corrected by human manganese superoxide dismutase-Plasmid/Liposome (SOD2-PL) intratracheal gene therapy. *Radiat Res* 2000;154:365-374.
19. Kang SK, Rabbani ZN, Folz RJ, *et al.* Overexpression of extracellular superoxide dismutase protects mice from radiation-induced lung injury. *Int J Radiat Oncol Biol Phys* 2003;57:1056-1066.
20. Batinic-Haberle I. Manganese porphyrins and related compounds as mimics of superoxide dismutase. *Methods Enzymol* 2002;349:223-233.
21. Batinic-Haberle I, Spasojevic I, Hambright P, *et al.* New class of potent catalysts of O2- dismutation. Mn(III)methoxyethylpyridyl- and methoxyethylimidazolylporphyrins. *Dalton Trans* 2004:1696-1702.
22. Batinic-Haberle I, Spasojevic I, Stevens RD, *et al.* Synthesis, characterization, and catalysis of O2.- dismutation. *J. Chem. Soc. Dalton Trans.* 2002:2689-2696.
23. Ferrer-Sueta G, Vitturi D, Batinic-Haberle I, *et al.* Reactions of manganese porphyrins with peroxynitrite and carbonate radical anion. *J Biol Chem* 2003;278:27432-27438.
24. Spasojevic I, Batinic-Haberle I, Fridovich I. Nitrosylation of manganese(II) tetrakis(N-ethylpyridinium-2-yl)porphyrin: a simple and sensitive spectrophotometric assay for nitric oxide. *Nitric Oxide* 2000;4:526-533.
25. Bowler RP, Sheng H, Enghild JJ, *et al.* A catalytic antioxidant (AEOL 10150) attenuates expression of inflammatory genes in stroke. *Free Radic Biol Med* 2002;33:1141-1152.
26. Sheng H, Enghild JJ, Bowler R, *et al.* Effects of metalloporphyrin catalytic antioxidants in experimental brain ischemia. *Free Radic Biol Med* 2002;33:947-961.
27. Mackensen GB, Patel M, Sheng H, *et al.* Neuroprotection from delayed postischemic administration of a metalloporphyrin catalytic antioxidant. *J Neurosci* 2001;21:4582-4592.
28. Piganelli JD, Flores SC, Cruz C, *et al.* A metalloporphyrin-based superoxide dismutase mimic inhibits adoptive transfer of autoimmune diabetes by a diabetogenic T-cell clone. *Diabetes* 2002;51:347-355.
29. Aslan M, Ryan TM, Adler B, *et al.* Oxygen radical inhibition of nitric oxide-dependent vascular function in sickle cell disease. *Proc Natl Acad Sci U S A* 2001;98:15215-15220.

30. Zhao Y, Oberley TD, Chaiswing L, *et al.* Manganese superoxide dismutase deficiency enhances cell turnover via tumor promoter-induced alterations in AP-1 and p53-mediated pathways in a skin cancer model. *Oncogene* 2002;21:3836-3846.
31. Tse HM, Milton MJ, Piganelli JD. Mechanistic analysis of the immunomodulatory effects of a catalytic antioxidant on antigen-presenting cells: implication for their use in targeting oxidation-reduction reactions in innate immunity. *Free Radic Biol Med* 2004;36:233-247.
32. Zhao Y, Chaiswing L, Oberley TD, *et al.* Mechanism based modulation of skin carcinogenesis by SOD mimetic in manganese superoxide dismutase difficient mice. *Free Radic Biol Med* 2004;Supp 1:S173.
33. Vujaskovic Z, Batinic-Haberle I, Rabbani ZN, *et al.* A small molecular weight catalytic metalloporphyrin antioxidant with superoxide dismutase (SOD) mimetic properties protects lungs from radiation-induced injury. *Free Radic Biol Med* 2002;33:857-863.
34. Maulik N, Das DK. Redox signaling in vascular angiogenesis. *Free Radic Biol Med* 2002;33:1047-1060.
35. Jung YD, Ellis LM. Inhibition of tumour invasion and angiogenesis by epigallocatechin gallate (EGCG), a major component of green tea. *Int J Exp Pathol* 2001;82:309-316.
36. Cao Y, Cao R. Angiogenesis inhibited by drinking tea. *Nature* 1999;398:381.
37. Atalay M, Gordillo G, Roy S, *et al.* Anti-angiogenic property of edible berry in a model of hemangioma. *FEBS Lett* 2003;544:252-257.
38. Roy S, Khanna S, Alessio HM, *et al.* Anti-angiogenic property of edible berries. *Free Radic Res* 2002;36:1023-1031.
39. Brakenhielm E, Cao R, Cao Y. Suppression of angiogenesis, tumor growth, and wound healing by resveratrol, a natural compound in red wine and grapes. *Faseb J* 2001;15:1798-1800.
40. Malafa MP, Fokum FD, Smith L, *et al.* Inhibition of angiogenesis and promotion of melanoma dormancy by vitamin E succinate. *Ann Surg Oncol* 2002;9:1023-1032.
41. Camphausen K, Menard C. Angiogenesis inhibitors and radiotherapy of primary tumours. *Expert Opin Biol Ther* 2002;2:477-481.
42. Batinic-Haberle I, Spasojevic I, Fridovich I. Tetrahydrobiopterin rapidly reduces SOD mimic, Mn(III) tetrakis(N-ethylpyridinium-2-yl)porphyrin. *Free Radic Biol Med* In Press.
43. Batinic-Haberle I, Benov L, Spasojevic I, *et al.* The Relationship Between Redox Potentials, Proton Dissociation Constants of Pyrrolic Nitrogen, and in Vitro and in Vivo Superoxide Dismutase Activities of Manganese(III) and Iron(III) Cationic and Anionic Porphyrins. *Inorg Chem* 1999;38:4011-4022.
44. Gorski DH, Beckett MA, Jaskowiak NT, *et al.* Blockage of the vascular endothelial growth factor stress response increases the antitumor effects of ionizing radiation. *Cancer Res* 1999;59:3374-3378.
45. Li CY, Shan S, Huang Q, *et al.* Initial stages of tumor cell-induced angiogenesis: evaluation via skin window chambers in rodent models. *J Natl Cancer Inst* 2000;92:143-147.

46. Lin P, Polverini P, Dewhirst M, *et al.* Inhibition of tumor angiogenesis using a soluble receptor establishes a role for Tie2 in pathologic vascular growth. *J Clin Invest* 1997;100:2072-2078.
47. Batinic-Haberle I, Liochev SI, Spasojevic I, *et al.* A potent superoxide dismutase mimic: manganese beta-octabromo-meso-tetrakis-(N-methylpyridinium-4-yl) porphyrin. *Arch Biochem Biophys* 1997;343:225-233.
48. Garcia-Barros M, Paris F, Cordon-Cardo C, *et al.* Tumor response to radiotherapy regulated by endothelial cell apoptosis. *Science* 2003;300:1155-1159.
49. Moeller B, Cao Y, Li C, *et al.* Radiation activates HIF-1 to regulate vascular radiosensitivity in tumors: role of reoxygenation, free radicals, and stress granules. *Cancer Cell* In Press.
50. Rugo RE, Secretan MB, Schiestl RH. X radiation causes a persistent induction of reactive oxygen species and a delayed reinduction of TP53 in normal human diploid fibroblasts. *Radiat Res* 2002;158:210-219.
51. Clutton SM, Townsend KM, Walker C, *et al.* Radiation-induced genomic instability and persisting oxidative stress in primary bone marrow cultures. *Carcinogenesis* 1996;17:1633-1639.
52. Burdon RH, Gill V, Rice-Evans C. Oxidative stress and tumour cell proliferation. *Free Radic Res Commun* 1990;11:65-76.
53. Szatrowski TP, Nathan CF. Production of large amounts of hydrogen peroxide by human tumor cells. *Cancer Res* 1991;51:794-798.
54. Oberley TD. Oxidative damage and cancer. *Am J Pathol* 2002;160:403-408.
55. Mikkelsen RB, Wardman P. Biological chemistry of reactive oxygen and nitrogen and radiation-induced signal transduction mechanisms. *Oncogene* 2003;22:5734-5754.
56. Chua CC, Hamdy RC, Chua BH. Upregulation of vascular endothelial growth factor by H2O2 in rat heart endothelial cells. *Free Radic Biol Med* 1998;25:891-897.
57. Shono T, Ono M, Izumi H, *et al.* Involvement of the transcription factor NF-kappaB in tubular morphogenesis of human microvascular endothelial cells by oxidative stress. *Mol Cell Biol* 1996;16:4231-4239.
58. Brauchle M, Funk JO, Kind P, *et al.* Ultraviolet B and H2O2 are potent inducers of vascular endothelial growth factor expression in cultured keratinocytes. *J Biol Chem* 1996;271:21793-21797.
59. Monte M, Davel LE, Sacerdote de Lustig E. Hydrogen peroxide is involved in lymphocyte activation mechanisms to induce angiogenesis. *Eur J Cancer* 1997;33:676-682.
60. Yasuda M, Ohzeki Y, Shimizu S, *et al.* Stimulation of in vitro angiogenesis by hydrogen peroxide and the relation with ETS-1 in endothelial cells. *Life Sci* 1999;64:249-258.
61. Mateo J, Garcia-Lecea M, Cadenas S, *et al.* Regulation of hypoxia-inducible factor-1alpha by nitric oxide through mitochondria-dependent and -independent pathways. *Biochem J* 2003;376:537-544.
62. Wellman TL, Jenkins J, Penar PL, *et al.* Nitric oxide and reactive oxygen species exert opposing effects on the stability of hypoxia-inducible factor-1alpha (HIF-1alpha) in explants of human pial arteries. *Faseb J* 2004;18:379-381.

63. Chandel NS, McClintock DS, Feliciano CE, *et al.* Reactive oxygen species generated at mitochondrial complex III stabilize hypoxia-inducible factor-1alpha during hypoxia: a mechanism of O2 sensing. *J Biol Chem* 2000;275:25130-25138.
64. Chandel NS, Maltepe E, Goldwasser E, *et al.* Mitochondrial reactive oxygen species trigger hypoxia-induced transcription. *Proc Natl Acad Sci U S A* 1998;95:11715-11720.
65. Semenza G. Signal transduction to hypoxia-inducible factor 1. *Biochem Pharmacol* 2002;64:993-998.
66. Garg AK, Aggarwal BB. Reactive oxygen intermediates in TNF signaling. *Mol Immunol* 2002;39:509-517.
67. Zhang Y, Chen F. Reactive oxygen species (ROS), troublemakers between nuclear factor-kappaB (NF-kappaB) and c-Jun NH(2)-terminal kinase (JNK). *Cancer Res* 2004;64:1902-1905.

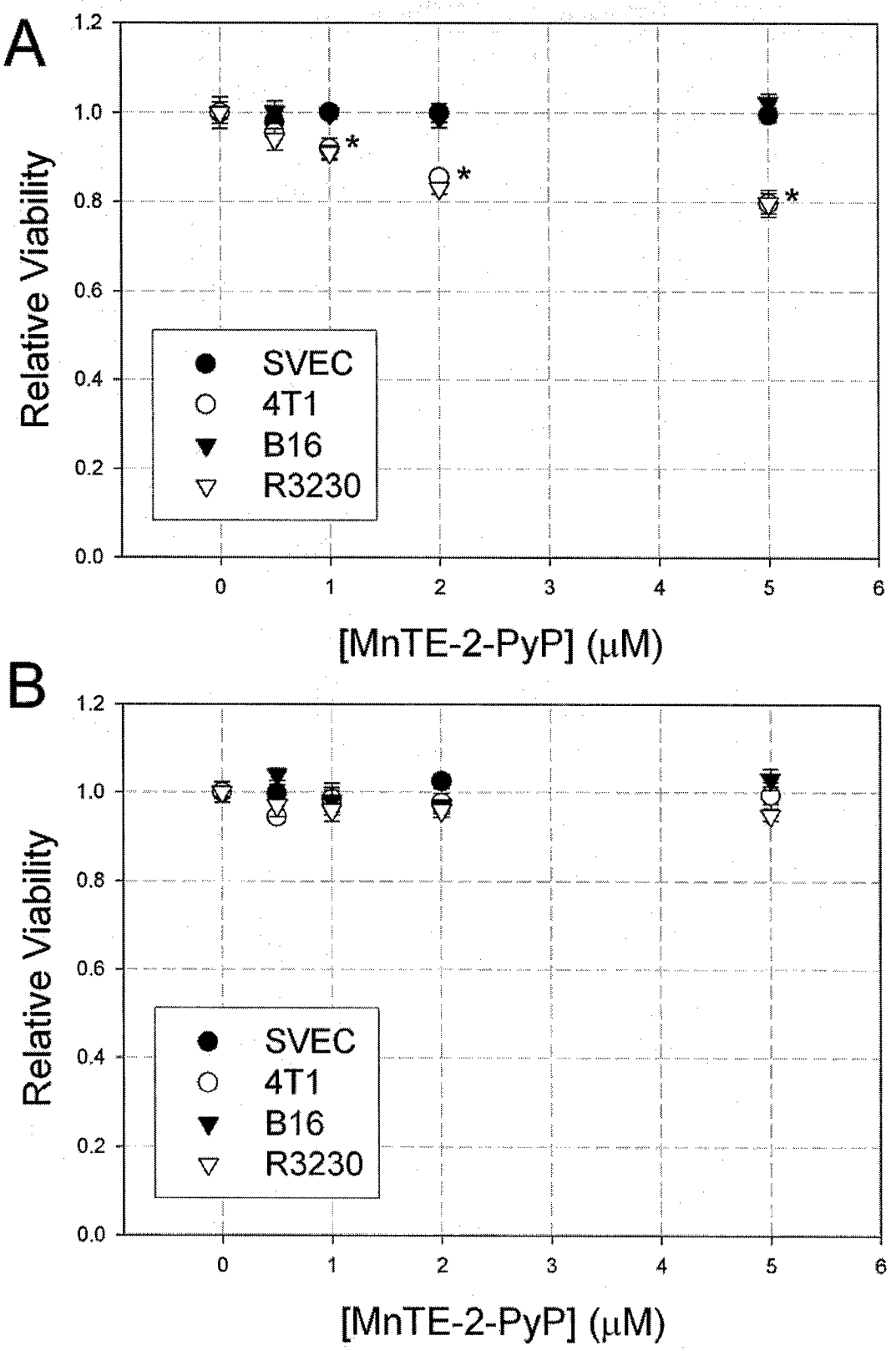
A
Relative Viability
1.2
1.0
0.8
0.6
0.4
0.2
0.0
0
1
2
3
4
5
6
SVEC
4T1
B16
R3230
*
*
*
[MnTE-2-PyP] (μM)
B
Relative Viability
1.2
1.0
0.8
0.6
0.4
0.2
0.0
0
1
2
3
4
5
6
SVEC
4T1
B16
R3230
[MnTE-2-PyP] (μM)

Figure 1

Figure 2.

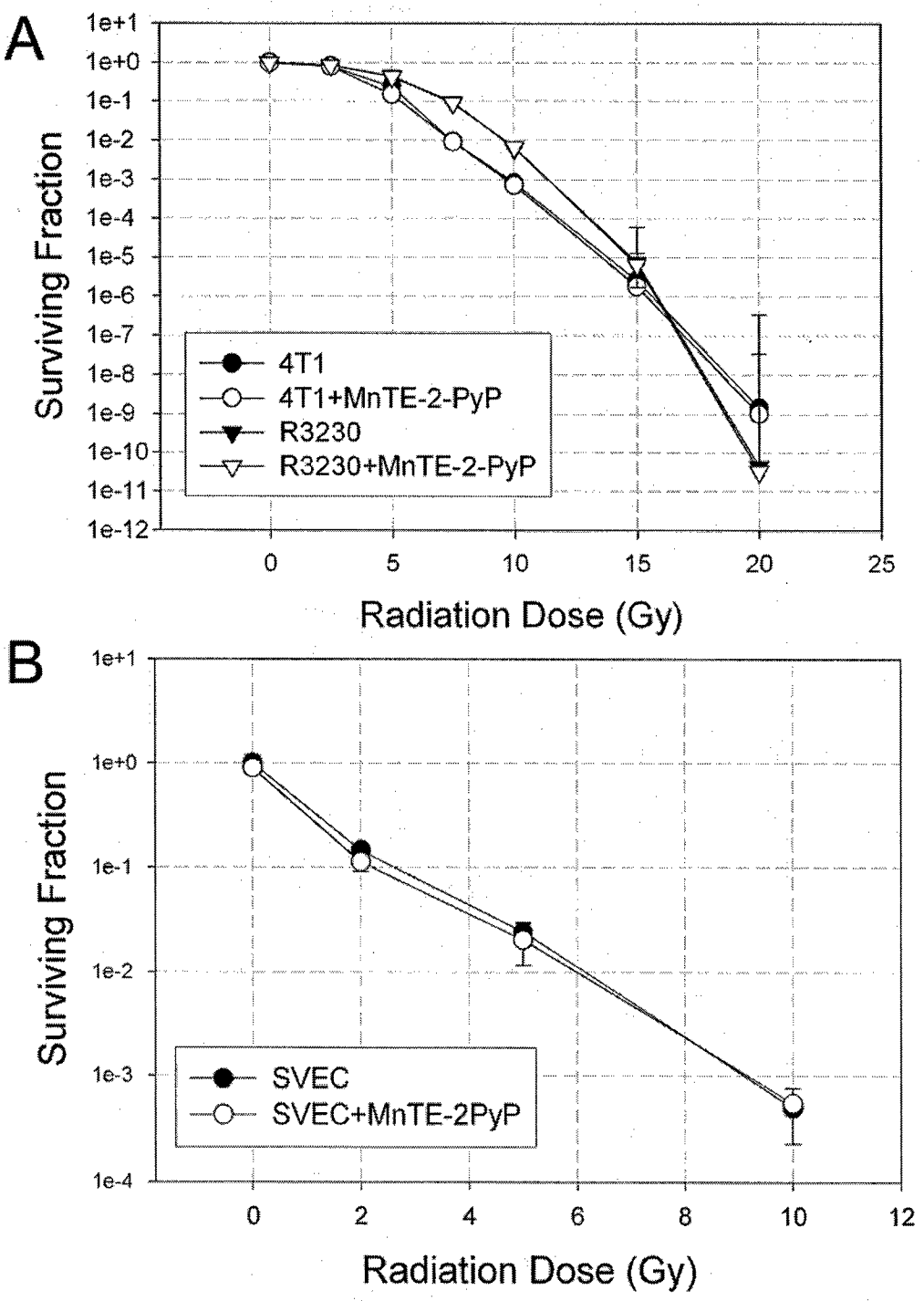
A
Surviving Fraction
1e+1
1e+0
1e-1
1e-2
1e-3
1e-4
1e-5
1e-6
1e-7
1e-8
1e-9
1e-10
1e-11
1e-12
4T1
4T1+MnTE-2-PyP
R3230
R3230+MnTE-2-PyP
0
5
10
15
20
25
Radiation Dose (Gy)
B
Surviving Fraction
1e+1
1e+0
1e-1
1e-2
1e-3
1e-4
SVEC
SVEC+MnTE-2PyP
0
2
4
6
8
10
12
Radiation Dose (Gy)

Figure 3.

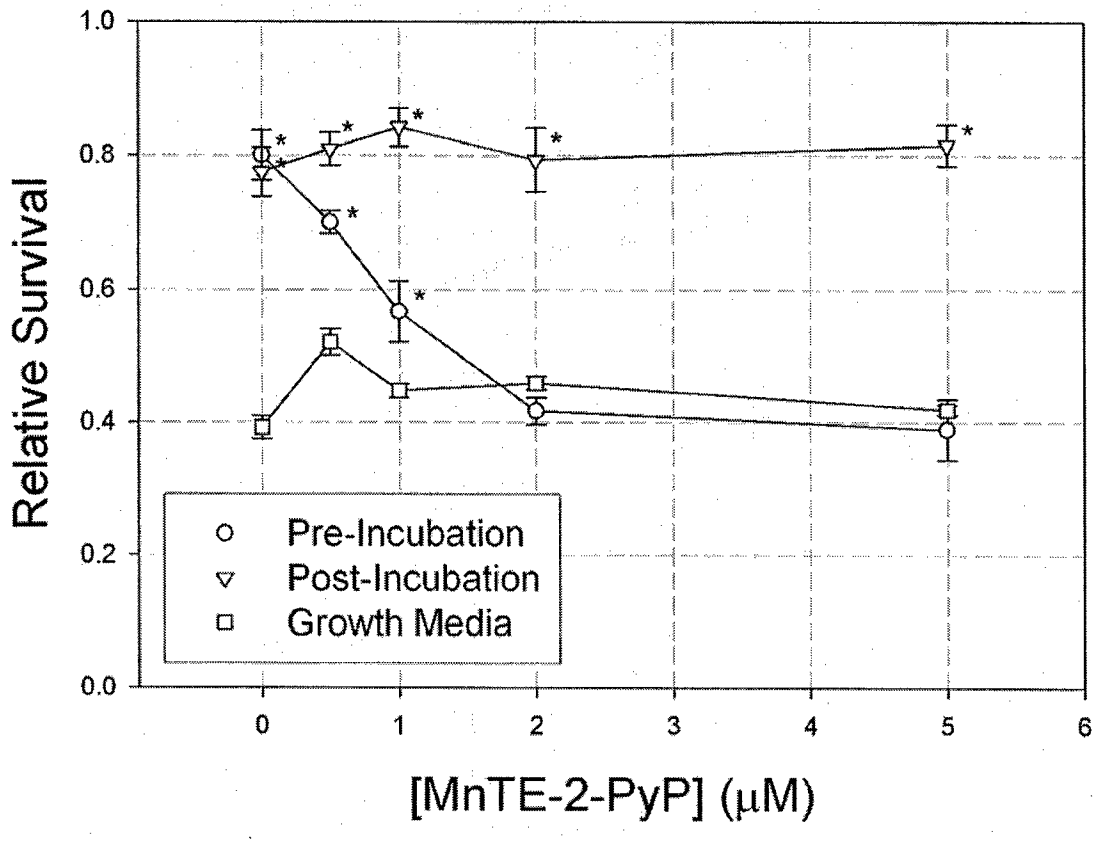
Relative Survival
1.0
0.8
0.6
0.4
0.2
0.0
0
1
2
3
4
5
6
[MnTE-2-PyP] (μM)
Pre-Incubation
Post-Incubation
Growth Media

Figure 4.

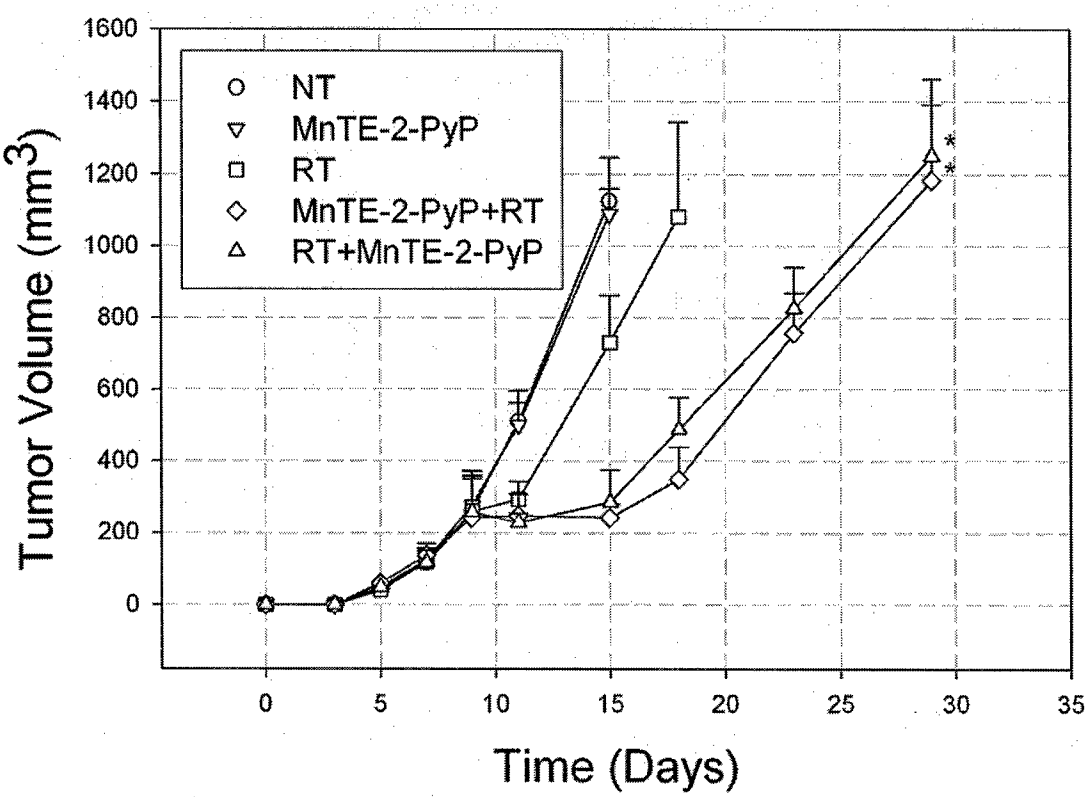
Tumor Volume (mm3)
1600
1400
1200
1000
800
600
400
200
0
NT
MnTE-2-PyP
RT
MnTE-2-PyP+RT
RT+MnTE-2-PyP
*
*
0
5
10
15
20
25
30
35
Time (Days)

Figure 5.

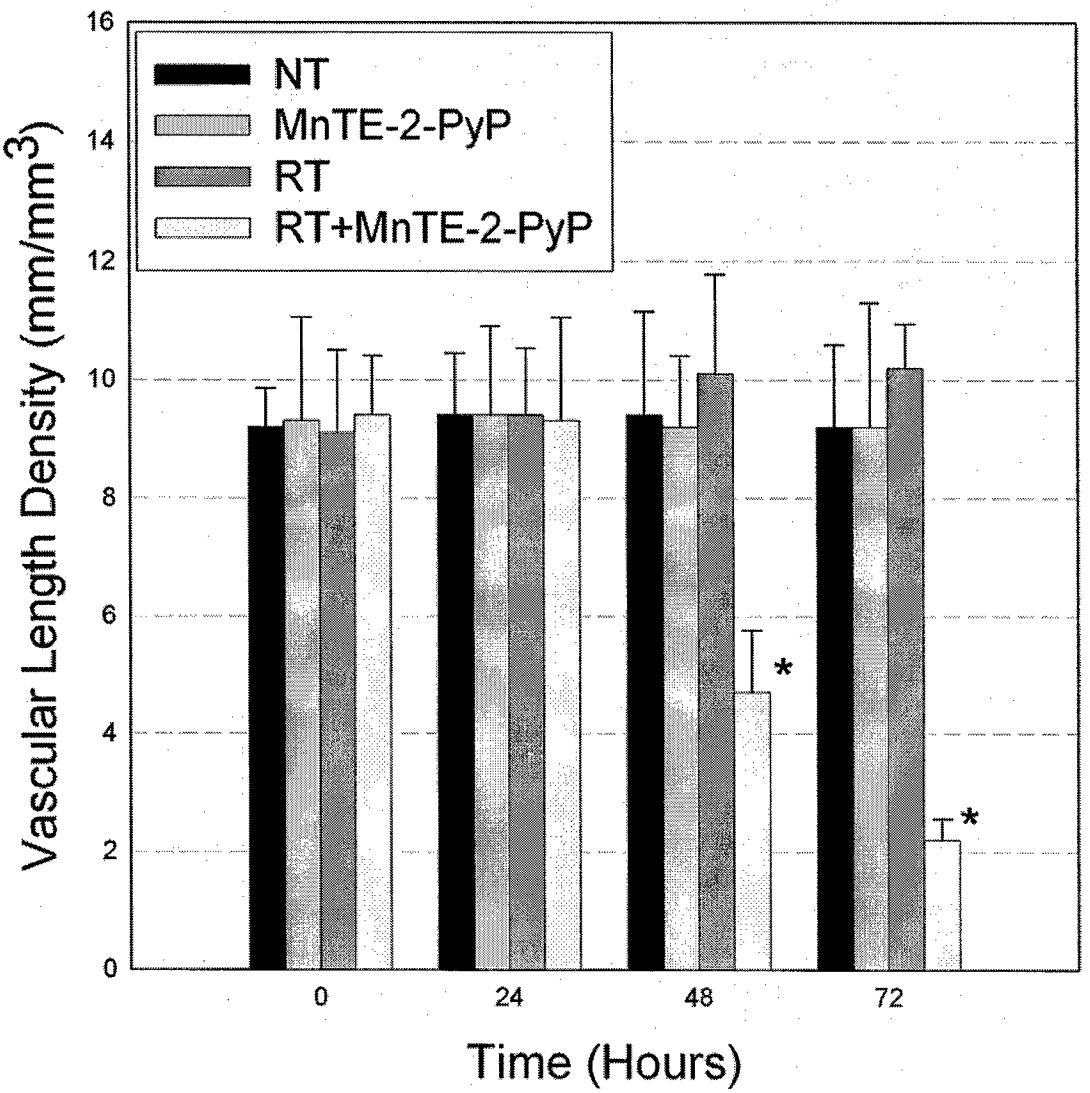
NT
MnTE-2-PyP
RT
RT+MnTE-2-PyP
Vascular Length Density (mm/mm3)
16
14
12
10
8
6
4
2
0
0
24
48
72
Time (Hours)
*
*

3. The 11th Annual Meeting of the Society for Free Radical Biology and Medicine, St. Thomas, Virgin Islands, November, 2004.

EFFECTS OF A CATALYTIC METALLOPORPHYRIN ANTIOXIDANT ON TUMOR RADIORESPONSIVENESS

Benjamin J. Moeller,[1] Ines Batinic-Haberle,[1] Ivan Spasojevic,[2] Zahid N. Rabbani,[1] Mitchell S. Anscher,[1] Zeljko Vujaskovic,[1] and Mark W. Dewhirst[1,3]
[1]Departments of Radiation Oncology[1] and Medicine[2], Duke University Medical Center, Durham, NC, USA

Studies have shown that a catalytic antioxidant, Mn(III) tetrakis(*N*-ethylpyridinium-2-yl)porphyrin (MnTE-2-PyP^{5+}), can suppress both late normal tissue radiation injury and tumor growth. We have herein investigated whether MnTE-2-PyP^{5+} may enhance tumor radiosensitivity by augmenting destruction of tumor vasculature. Various rodent tumor and endothelial cells lines were exposed to MnTE-2-PyP^{5+} and assayed for viability and radiosensitivity *in vitro*. Next, tumors were treated with radiation and MnTE-2-PyP^{5+} *in vivo*, and the effects on tumor growth and vascularity were monitored. *In vitro*, MnTE-2-PyP^{5+} had minimal impact on the viability and radiosensitivity of various tumor and endothelial cell lines. However, it significantly inhibited the ability of tumor cells to secrete factors capable of rescuing irradiated endothelial cells. *In vivo*, combined treatment with radiation and MnTE-2-PyP^{5+} resulted in synergistic anti-tumor effects, irrespective of treatment sequencing or the duration of drug dosing. Co-treatment of tumors also achieved synergistic tumor devascularization, resulting in near complete destruction of the pre-existing tumor vasculature. These studies support the conclusion that MnTE-2-PyP^{5+} can protect normal tissues from radiation injury while improving tumor control, through augmenting radiation-induced damage to the tumor vasculature.

4. Gordon Conference, Ventura 2004 02-05-04

Ines Batinic-Haberle, Manganese porphyrins as catalytic antioxidants

The data are presented as a part of talk under the title "***Manganese porphyrins as catalytic antioxidants***" given at Gordon Conference on Oxygen Radicals In Ventura, 2004.

The tumor anti-angiogenic effect of MnTE-2-PyP^{5+} in mouse

Moeller et al, in preparation

Intravital microscopy of dorsal skinfold window chamber